European Polymer Journal 47 (2011) 2033–2052

Contents lists available at SciVerse ScienceDirect

European Polymer Journal

journal homepage: www.elsevier.com/locate/europolj

Macromolecular Nanotechnology – Review

Polymers in conventional and alternative lithography for the fabrication of nanostructures

Canet Acikgoz [a,b], Mark A. Hempenius [a], Jurriaan Huskens [b,*], G. Julius Vancso [a,*]

[a] Materials Science and Technology of Polymers, MESA+ Institute for Nanotechnology, University of Twente, P.O. Box 217, 7500 AE Enschede, The Netherlands
[b] Molecular Nanofabrication Group, MESA+ Institute for Nanotechnology, University of Twente, P.O. Box 217, 7500 AE Enschede, The Netherlands

ARTICLE INFO

Article history:
Received 18 February 2011
Received in revised form 4 July 2011
Accepted 31 July 2011
Available online 19 August 2011

Keywords:
Polymer resists
Conventional lithography
Alternative lithography
Patterning
Colloidal assembly
Nanoimprint lithography

ABSTRACT

This review provides a survey of lithography techniques and the resist materials employed with these techniques. The first part focuses on the conventional lithography methods used to fabricate complex micro- and nano-structured surfaces. In the second part, emphasis is placed on patterning with unconventional lithography techniques such as printing, molding, and embossing, and on their development into viable, high-resolution patterning technologies.

Contents

* Corresponding authors. Tel.: +31 53 4892995; fax: +31 53 4894645 (J. Huskens), tel.: +31 53 4892974; fax: +31 53 4893823 (G.J. Vancso).
E-mail addresses: J.Huskens@utwente.nl (J. Huskens), g.j.vancso@utwente.nl (G.J. Vancso).

0014-3057
doi:10.1016/j.eurpolymj.2011.07.025

1. Introduction

Nanofabrication is the process of making functional structures with patterns having minimum dimensions of approximately <100 nm. Methods used to fabricate nanoscale structures and nanostructured materials are labeled as 'top-down' and 'bottom-up'. Photolithography and scanning beam lithography for the creation of patterns in the micrometer and nanometer range are so called top-down approaches, in which the structure is imposed on the substrate by a mask or by direct writing. When the surface is structured by self-assembly of small building blocks such as copolymers, vesicles, micelles, or particles, the 'bottom-up' term is generally used [1]. Similarly, direct 'one-to-one' manipulation of atoms, molecules and nanoscale molecular objects is also referred to as 'bottom-up' assembly.

The top-down techniques including photolithography [2,3] and scanning beam lithography [4] are known as conventional lithography. These techniques have relatively high cost and/or expose substrates to high energy radiation and relatively high temperatures. Alternative techniques have emerged to pattern relatively fragile materials, such as organic materials other than photoresists. These techniques are often employed in research and allow fast prototyping of nanostructures. Unconventional nanofabrication techniques explored are molding [5], embossing [6,7], printing [8,9], scanning probe lithography [10–12], edge lithography [13–16], and self-assembly [17,18]. The first three techniques are top-down approaches whereas scanning probe lithography, edge lithography and self-assembly bridge 'top-down' and 'bottom up' strategies for nanofabrication,

Critical issues such as resolution, reliability, speed, and overlay accuracy need to be considered in developing new lithography techniques. Unconventional nanofabrication techniques offer alternatives to photolithography and create opportunities for fabrication on nonplanar surfaces and over large areas. Moreover, they have the potential to be low-cost for manufacturing and they are easier to operate and are applicable to biological materials.

In both approaches, polymers play an important role owing to their lengthscale, their processability, low cost, tunable properties, diverse functionalities and (if block copolymers are used) microphase separation. These features make polymers versatile materials for nanoscale UV lithography [19] and imprint lithography [20] as examples of existing top-down techniques where these materials are utilized either as a resist layer or as a substrate. Polymers have been widely used in patterning of surfaces by top-down "soft lithography", which, according to Nuzzo et al., refers to a group of techniques using "elastomeric stamps, molds, and conformable photomasks" for pattern replication [21,9]. Regarding the use of polymers in top-down techniques, each specific technique has its own merits, challenges and limitations.

This review surveys lithography techniques and materials, in particular polymers used in these lithographic techniques. Herein, the first part focuses on the conventional lithography techniques used to fabricate complex micro- and nano-structured surfaces. In the second part, the focus lies on patterning with unconventional lithographic methods such as printing, molding, and embossing to fabricate nanostructures which are central to the development of a number of existing and emerging technologies.

2. Conventional lithography

Conventional techniques for nanofabrication are commercially available and widely implemented in manufacturing. These conventional approaches have their limitations such as high cost and the difficulty in accessing the facilities to use them. There are two dominant methods for conventional lithography: photolithography and particle beam lithography such as electron beam lithography and ion beam lithography.

2.1. Photolithography

Photolithographic methods all share the same operational principle: exposure of an appropriate material to electromagnetic radiation to modify the solubility of the material as a result of chemical changes in its molecular structure, followed by developing of the material (Fig. 1a). The exposed photoresist is immersed in solvents that dissolve the exposed (positive photoresist) or unexposed (negative photoresist) regions to provide access to the surface of the substrate. Pattern transfer is achieved by an etching process [22].

Most efforts in lithography have been directed at shrinking the lateral dimensions of the features, and different resolution enhancement approaches (projection and immersion optics, phase-shifting masks) have been developed [3,23]. In current semiconductor nanofabrication, photolithography can pattern 37 nm-wide features with 193-nm wavelength [24]. In order to extend the resolution capabilities of 193-nm, the semiconductor industry found another potential route to scale the effective wavelength via immersion lithography. In immersion lithography, imaging resolution is improved by increasing the refractive index of the medium between the imaging lens and the imaging plane [1,25]. The use of a coupling medium with a refractive index greater than that of air between the last lens element and the photoresist provides an increase in the depth of focus and also allows lenses with larger capture angles to be used in the imaging system. This adaptation of this technology into high volume manufacturing was achieved by solving the technical problems such as

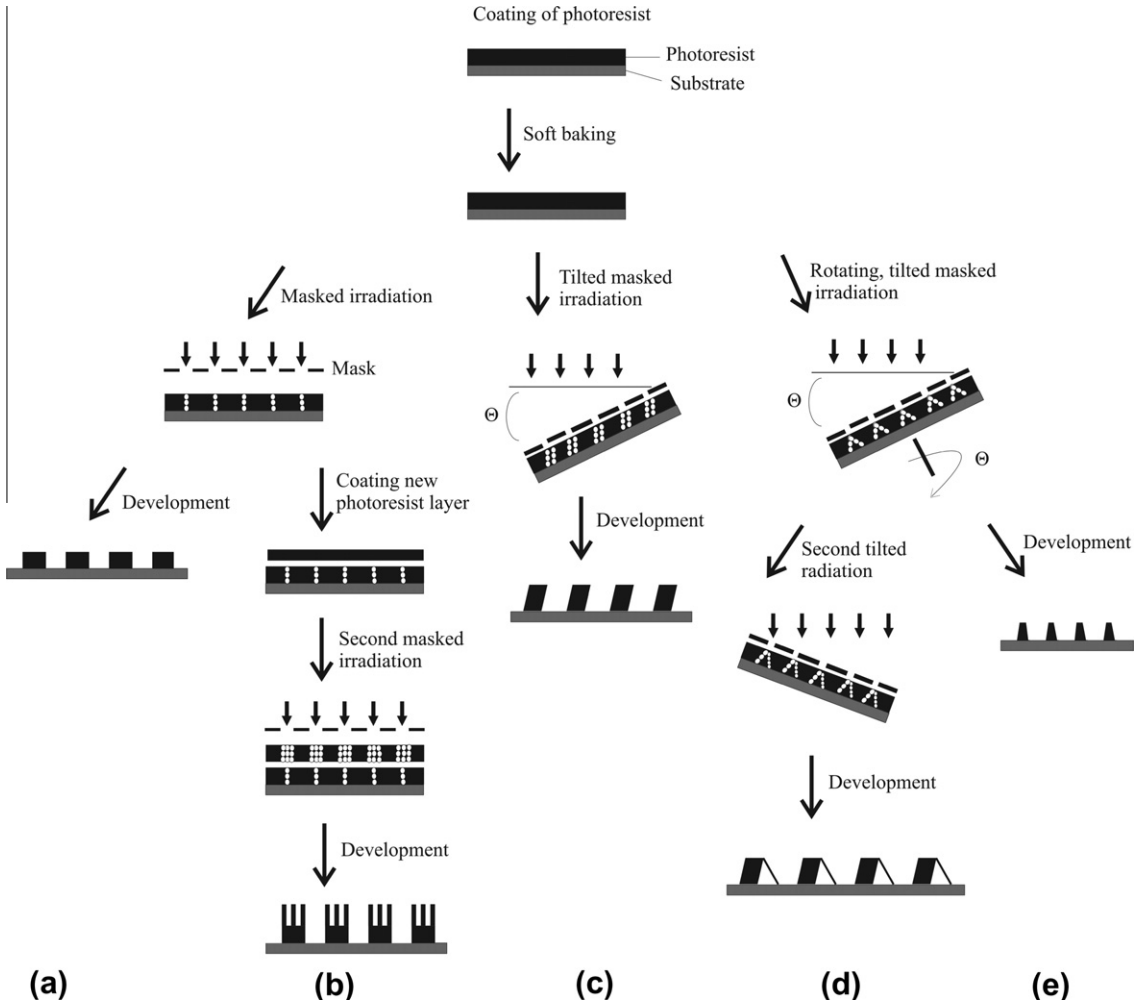

Fig. 1. Photolithographic methods using masked irradiation and a negative photoresist material: (a) Patterning by single exposure, (b) patterning by layer-by-layer coating and exposure, (c) tilted patterning by single inclined exposure, (d) patterning by double inclined exposure, (e) tapered patterns by rotating tilted exposure. Reproduced with permission from [26]. Copyright © 2008 American Chemical Society.

the impact of water on photoresist materials or fabrication of complex lenses. For example, high-index immersion lithography employing a lutetium aluminum garnet high-index last lens element and alicyclic hydrocarbon high-index immersion fluids was shown to be capable of sub-30 nm half-pitch imaging [25].

Recently, photolithographic approaches have been extended to generate more complex structures including high aspect ratio, tilted, suspended, or curved geometries (Fig. 1) [26]. In conventional lithography, the mask and resist film are perpendicularly aligned with respect to the irradiation source. By tilting the mask and resist film with respect to the beam using a tilting stage, inclined structures can be fabricated (Fig. 1c). Han et al. showed the generation of bridges, embedded channels, and V-grooves with aspect ratios >4 using SU-8 (epoxy-based negative photoresist) and a conventional UV mask aligner (Fig. 2a) [27]. More complex 3D structures can be fabricated with three or four times inclined UV exposures along different axes (Fig. 1d) [28,29]. Inclined micro-pillars with an aspect ratio of 20 (Fig. 2b) were fabricated using a two-axes exposure method with four backside exposures but the multi-exposure process can generate heavy UV dose domains which could cause distortions. Tapered structures with nonvertical sidewalls can be also obtained if the photomask and substrate with photoresist are tilted and rotated simultaneously during irradiation as shown in Fig. 1d and the SEM image in Fig. 2c [27].

2.2. Serial writing with charged particles

Serial writing with electrons or ions is a lithographic technique with low throughput, high cost and only suited for small area fabrication. These techniques provide, however, flexibility in feature design making them attractive in academic research.

2.2.1. Electron beam lithography

In typical e-beam lithography, a beam of electrons is used to expose an electron sensitive resist. The electrons

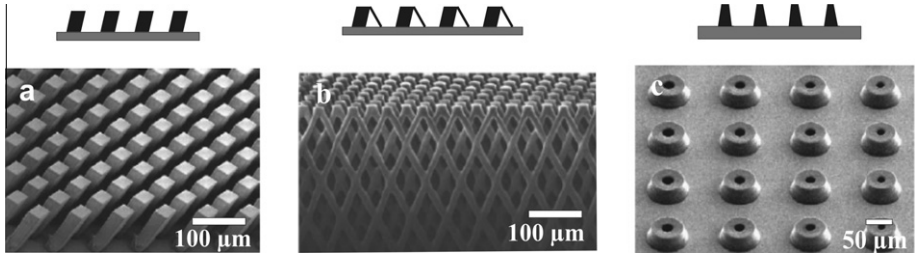

Fig. 2. SEM images of (a) tilted SU-8 patterns, (b) patterns by double inclined exposure, (c) tapered patterns by rotating tilted exposure. (a, c) Reproduced with permission from [27]. Copyright © 2004 Elsevier B.V. (b) Reproduced with permission from [28]. Copyright © 2004 Springer Science+Business Media.

generate secondary electrons with relatively low energy to form free radicals and radical cations, which interact with the surface of a layer of resist, such as poly(methyl methacrylate) (PMMA). Interaction of the electron beam with the resist causes local changes in its solubility, and in the case of PMMA, the electrons will locally induce chain scissions that makes the polymer soluble in a developer. PMMA was one of the first polymers recognized to exhibit sensitivity to electron beam radiation and is nowadays the most frequently used polymer in e-beam lithography [26]. ZEP (Nippon Zeon Co.) which consists of a copolymer of α-chloromethacrylate and α-methylstyrene is a relative newcomer to e-beam lithography [30], and shows better etch resistance compared to PMMA [31].

Even though electron wavelengths on the order of 1 Å can be achieved, the resolution is limited because of the electron scattering of primary and secondary electrons in the resist. Nevertheless, patterns with features as small as ~50 nm can be generated by this technique [32].

E-beam lithography is impractical for mass production because of long writing times. Therefore, it is mainly used to produce photomasks in optical lithography or to produce small numbers of nanostructures for research purposes. It is also used in the areas where optical lithography fails such as for the fabrication of high frequency GaAs field-effect transistor (FET) devices that require a resolution down to ~100 nm [33].

2.2.2. Ion beam lithography

This method includes a variation of the electron beam lithography technique, using a focused ion beam (FIB) instead of an electron beam. High energy ions, such as Ga^+, H^+, or He^+ are able to penetrate a resist material with well defined paths. The penetration depth depends on the ion energy. Ion–electron interactions do not result in significant deviation of the trajectory of the ion from the straight line path. Therefore high aspect ratio structures with vertical side walls can be fabricated. Similar to e-beam writing, the low energy secondary electrons initiate chemical reactions [26].

The utilization of a focused mega-electron-volt (MeV) proton beam to write accurate high-aspect-ratio walls of 30 nm width with sub-3 nm edge smoothness has been reported [34]. Typically, a MeV proton beam is focused to a sub-100 nm spot size and scanned over a suitable resist material. When the proton beam interacts with matter it follows an almost straight path. The secondary electrons induced by the primary proton beam have low energy and therefore limited range, resulting in minimal proximity effects. These features enable smooth three-dimensional structures to be directly written into resist materials. The technique is named *p-beam writing* [34].

3. Alternative lithographies

Photolithography has circumvented many limitations during its development and is widely used to fabricate nanostructures [35,36]. However, the limitations based on the physics of diffraction and interactions of high energy photons are hard to overcome. This technique cannot easily be performed on polymeric or curved substrates and cannot pattern large areas with high resolution in a single step. It also has the disadvantage of high capital and operational cost. Hence in order to accomplish smaller features at a lower cost, new patterning techniques are being explored and developed. Some of the oldest and conceptually simplest forms of plastics macroscale processing (embossing, molding, stamping, or printing) are now being reexamined for their potential adaptation to nanofabrication. In the molding technique, the surface relief of a hard stamp or mold is transferred into a soft material. Several methods have been developed in the past decade to obtain micro- and nano-structured polymer surfaces using molding or related strategies. Some of them are (i) temperature-based processing (hot embossing or nanoimprint lithography (NIL) and thermal injection molding of thermoplastic polymers), (ii) light-initiated polymerization (UV-NIL and step-and-flash NIL), (iii) soft lithography, (iv) solvent-based processing, and (v) nanosphere lithography. Fig. 3 gives an overview of the processing steps involved.

3.1. Mold fabrication

Mold fabrication is the most time- and cost-consuming step and one of the largest limitations in industrial application [37]. For this reason, a master is fabricated and copies of the master in other hard materials are preferentially used as molds for imprinting. High resolution 3D stamps are fabricated by e-beam lithography and dry etching, while shallow stamps can be obtained by e-beam lithography and metal lift-off [38]. A widespread choice of stamp material is Si with an oxide layer on top [20,39]. Masters of Si are fabricated by reactive ion etching techniques [40] or deposition of nickel and other metals on patterned resist substrates. Small features with sub-20 nm dimensions have been achieved by electron beam lithography

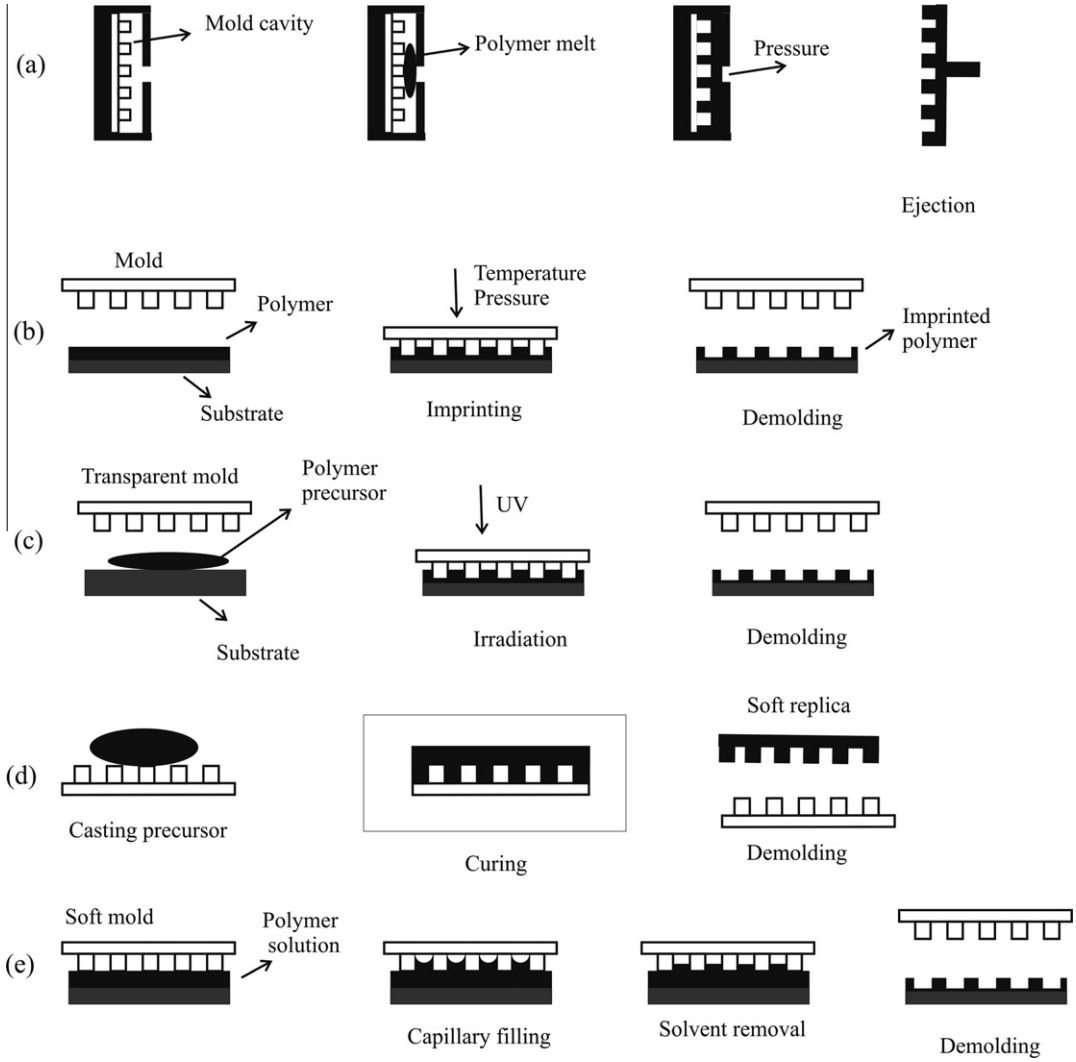

Fig. 3. Different alternative lithographic processes. (a) Injection molding, (b) hot embossing (thermal NIL), (c) UV-NIL, (d) soft lithography, (e) solvent-assisted molding. Reproduced with permission from [26]. Copyright © 2008 American Chemical Society.

and lift off [41]. An optimized double-layer resist system allowed the formation of a Cr etching mask with feature sizes of 15–20 nm in diameter. However, the metal roughness was found to be a problem for sizes below 10 nm due to the granularity of the evaporated metal [42]. Selecting the mold material should be carefully done and issues such as hardness, compatibility with other microfabrication processing methods and thermal expansion coefficients must be considered. Diamond [43] and lithium [44] have been investigated as potential mold materials for NIL by some groups. Taniguchi et al. used a spin-on-glass (SOG) material, which is almost the same as quartz in composition, as a material for hard stamps [45]. The SOG acted as a positive-tone electron beam resist and nanopatterns were fabricated by using e-beam lithography (EBL). The obtained pattern was directly usable as a nanoimprint mold without the risk of etching.

EBL has been established as a useful method for production of masters but so far lacks the commercial viability due to the high cost related to the exposure procedure. Etching of poly(tetrafluoroethylene) (PTFE) using synchrotron radiation also proved to be a feasible method for the 3D fabrication of masters [46]. Owing to its thermostability, resistance to chemicals and its very low adhesion, PTFE may be one of the most suitable materials for molding polymers, even though PTFE is notoriously difficult to process. Using synchrotron radiation, however, processing of 1000 μm height structures takes about 10 min, much shorter than achieved by X-ray lithography. Due to the directional emission of synchrotron radiation, high aspect ratio structures can be easily created.

In order to facilitate mold release, antisticking surface coatings are being used. These layers lower the surface tension of the mold surface and reduce adhesion. Different strategies can be employed: (i) use of fluoropolymer films deposited (noncovalently bonded) on the stamps with the help of a plasma treatment; (ii) treatment of silicon masters with perfluorosilanes, e.g. 1*H*,1*H*,2*H*,2*H*-perfluorode-

cyltrichlorosilane [47]; and (iii) treatment of Ni or alumina stamps with fluorinated alkyl phosphoric acid derivatives [48]. Alternatively, molds made of fluoropolymers, such as PTFE, can be used. These molds are fabricated by casting a fluoropolymer solution on the master followed by drying, or imprinting the fluoropolymer melt.

One of the many advantages of molding is that it does not use light energy beams, and therefore, its resolution is not limited by the effects of wave diffraction, scattering, or back scattering from the substrate [36]. The same mold can be used several times to fabricate nanostructures which makes it a low cost technique. The availability of a suitable mold and the possibility of removing the molded material from it without damage are the prerequisites for molding.

3.2. Nanoimprint lithography

The principle of nanoimprint lithography [7,20,39] (hot embossing) and thermal injection is that a hard mold containing nanoscale features on its surface is used to deform a thermoplastic polymer deposited on the wafer substrate under controlled temperature and pressure (Fig. 3b) [49]. Increase of the temperature of the polymer reduces the viscosity of the material so that pressure application causes the polymer melt to flow into the cavities of the mold. The subsequent cooling of the system freezes the pattern on the target surface, thus providing a negative copy of the master.

Injection molding and hot embossing differ in their applications and process conditions. In injection molding, a polymer melt is injected at high pressure into a cavity where it cools and hardens (Fig. 3a). In NIL, polymer sheets are compressed between the plates of an embossing press against the mold. Since imprint lithography makes a replica of surface patterns, the resist materials used in imprinting should be deformable under the applied pressure [20,50]. In NIL, typically a thermoplastic material is used as the imprinting resist and a suitable imprint temperature is chosen which is above the glass transition temperature of the material. It has been shown that an optimal imprinting temperature is 70–80 °C above the T_g of the material used [51], to insure the polymer has a sufficiently reduced viscosity so that imprinting can be performed at a reasonable pressure. Raising the temperature above the T_g of the polymer causes a significant drop in both Young's modulus and the viscosity. The viscosity of a polymer material not only depends on the temperature, but also strongly on the polymer molar mass. In practice, low-molecular weight polymers can be imprinted at lower temperatures, lower pressures, or within shorter times [52]. A high imprint pressure is needed for resist viscosities of 1000 Pa s and more to provide conformal contact between substrate and stamp over large areas. A thin polymer layer can be chosen where cavities are only partially filled, and thick layers can be used for the integration of lenses and microfluidic channels [53–55]. A good choice of process parameters such as height, pressure, thickness and temperature is always required to imprint polymers.

NIL can be used to mold a variety of polymeric materials and pattern features as small as ~5 nm [56] and aspect ratios of up to ~20 nm [57]. Arrays of 10 nm diameter and 40 nm period holes in PMMA on either silicon or gold substrates, and 6 nm diameter and 65 nm period holes in PMMA on silicon substrates have been fabricated by NIL (Fig. 4a) [56]. NIL was used together with optical lithography to fabricate silicon quantum dot wires, which showed the same behavior as those fabricated using conventional electron-beam lithography. In addition, nanoimprint lithography was used to fabricate nanocompact disks with 10 nm features and 400 Gbits/in^2 data density—nearly three orders of magnitude higher than current CDs (Fig. 4b) [56]. Materials that have been patterned successfully include biomolecules [58], block copolymers [59]

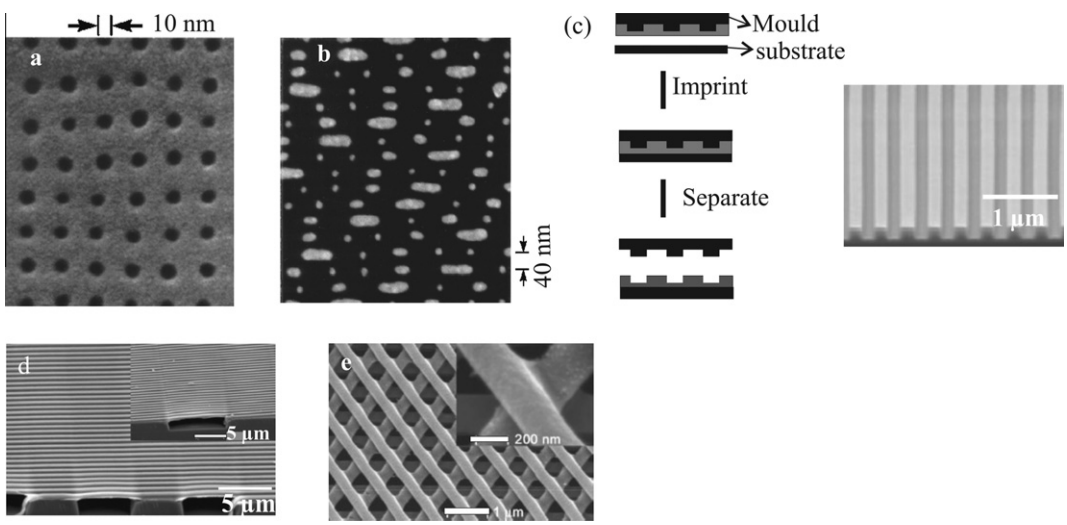

Fig. 4. (a) SEM image of holes imprinted into PMMA [56]. (b) SEM image of a 40 nm track of a nano-CD fabricated by NIL and metal lift-off [56]. (c) Schematic of reverse nanoimprint and SEM of reverse imprinted PMMA gratings with 350 nm line width/spacing [75]. (d) SEM image of polycarbonate grating structures imprinted with reverse imprinting [75]. (e) SEM image of an imprinted three-layer nanostructure, using three different polymers [75]. Reproduced with permission from [56,75]. Copyright © 1997, 2002 American Vacuum Society.

and conducting polymers [60]. This process has been extended to pattern components for a range of microelectronics, optical, and optoelectronic devices [61]. The fabrication of 60-nm channel metal-oxide-semiconductor field-effect transistors on whole 4-in wafers using NIL was presented. The nanotransistors exhibited excellent operational characteristics across the wafer [62].

The availability of polymers such as PMMA and polystyrene (PS) with a range of molar masses M_w and different polydispersities is an advantage for thermal NIL, and rheological characterization of the thermoplastic materials is available [63]. These materials are, however, not fully optimized for the special requirements of the NIL process. One of the most important requirements of the polymers used for NIL is that they should provide excellent mold releasing properties during the demolding process. Commercially available polymers can hardly satisfy this requirement. During imprinting of high aspect ratio patterns, the imprinted polymer tends to adhere to the mold, creating pattern defects even if the mold surface is treated with an antisticking layer.

Methacrylate based polymers and copolymers containing aromatic components were synthesized as alternatives to PMMA and they are commercially available with T_g values of 60 and 115 °C, respectively (mr-I 7000 and mr-I 8000 of micro resist technology GmbH). Thermally curing polymers based on allyl ester prepolymers, which are all superior to PMMA in terms of etch resistivity, have been developed for NIL [64,65].

A higher dry etching resistance is desirable if the imprinted polymer pattern is to be used as a mask for further pattern transfer. Adding a Si-containing material can also address this problem [66]. A number of siloxane copolymers have been investigated for use as NIL resists, including poly(dimethylsiloxane)-*block*-polystyrene (PDMS-*b*-PS), poly(dimethylsiloxane)-*graft*-poly (methyl acrylate)-*co*-poly(isobornyl acrylate) (PDMS-*g*-PMA-*co*-PIA), and PDMS-*g*-PMMA [67]. One of the biggest advantages of using siloxane polymers as an NIL resist is that they can offer much improved etching resistance when exposed to oxygen plasma since the products of chemical etching with oxygen plasmas are non-volatile and do not desorb from the surface [68].

The application of poly(ferrocenylsilane)s (PFS) as a new type of imprint resist has recently been reported [69]. Poly(ferrocenylsilane) (PFS) [70,71] containing iron and silicon atoms in the main chain, is a class of organometallic polymers, which are converted to oxides upon exposure to oxygen plasmas [68]. Stable, homogeneous high molar mass poly(ferrocenylmethylphenylsilane) (PFMPS) films obtained by spin coating were imprinted and the resulting patterns were further transferred into the substrate by a reactive ion etching process. It was shown that PFMPS, because of its excellent etch contrast vs silicon, can be used as a single step resist since there is no need for metal lift-off.

Nanoimprint lithography has made great progress in a relatively short time but there are still some challenges related to this technique, one of which is the lifetime of the mold. Nanoimprint molds have to be replaced after ~50 consecutive imprints. High pressures and heating and cooling cycles cause stress and wear on the nanoimprint mold. Room temperature nanoimprint lithography [72] has been developed to overcome this problem. Spin-on-glass [73] or hydrogen silsesquioxane [74] have been used as resist materials in room temperature nanoimprint lithography. Some different approaches have also been developed targeting the problems mentioned above. One of the approaches is reverse nanoimprint lithography [66] which employs a polymer film spin-coated onto the mold rather than on the substrate. The produced film can be transferred from the mold to the substrate by NIL (Fig. 4c). This technique was performed by using PMMA and Fig. 4c shows imprinted PMMA patterns with 350 nm line spacing. This technique can also be used to transfer patterns onto substrates that are not suitable for spin-coating or have surface topographies, which has been a long-standing problem in imprint-based lithography [75]. Multilayer resist approaches with a thick planarization layer on top of the non-flat substrate have been used to solve this problem but these approaches require complex processes with multiple steps and need deep etching through the thick planarization layer [76]. Reverse imprinting has solved this problem very efficiently. Fig. 4d shows polycarbonate grating structures reverse imprinted over etched features on a Si substrate which could have potential application in chemical and biological analysis [75]. This technique also offers the fabrication of three-dimensional structures by a layer-by-layer approach. Fig. 4e demonstrates an imprinted three-layer nanostructure, using three different polymers. The imprinting results depend on several parameters such as T_g of the polymers, film thickness, width and height of the features on the substrate, and mechanical properties of the polymers [75].

A high viscosity of the polymer film presents another challenge for nanofabrication using NIL. An optimal pattern size and feature density should be provided for NIL [77]. Embossing micrometer-scale features can be more challenging than nano-scale features since filling large areas within the mold requires more lateral displacement of the polymer than smaller features and thus the processing time increases. The flow phenomena have been investigated by use of specific test patterns, for example negative and positive stamps or stamps with different pattern sizes. During imprinting, the resist is displaced by squeeze flow and capillary forces [78]. The thickness of the residual layer can also vary across the imprinted region depending on the pattern density or layout of the patterns. Residual layer non-uniformities present a challenge for transferring the pattern uniformly into the underlying substrate [1].

Combination of NIL with other patterning techniques allows the fabrication of 3D structures [79]. It has been shown that performing a step of imprinting into a PMMA film and utilizing that prepatterned polymer layer as a resist for X-ray lithography provides a flexible method to fabricate a wide class of complex small-scale 3D structures (Fig. 5).

NIL has also been combined with photolithography to replicate structures in negative tone resists by introducing a hybrid mask concept which is made of UV transparent material and acts both as a NIL mold and as a photolithog-

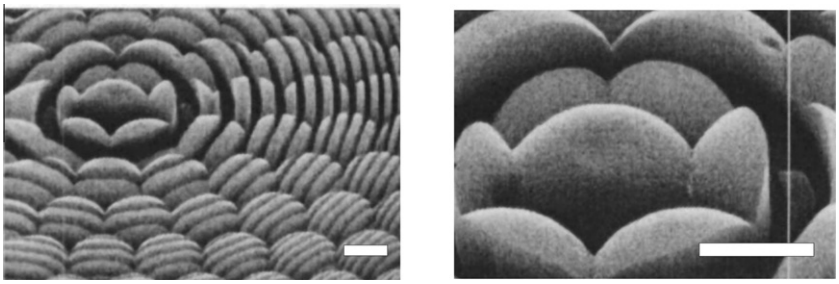

Fig. 5. 3D patterns obtained by combining X-ray lithography with NIL. The scale bar represents 10 μm. Reproduced with permission from [79]. Copyright © 2004 American Vacuum Society.

raphy mask [66]. A further improvement has been made by placing a metal layer on top of the mold so that exposure of the resist layer underneath could be prevented while unexposed residual layer could be removed easily in a developer solution. This can eliminate the residual layer removal step in NIL completely and could simultaneously solve the problem associated with the non-uniformity of the residual layer.

3.3. Ultraviolet-assisted nanoimprint lithography (UV-NIL)

UV-NIL [80] makes use of UV-curable polymeric materials for imprinting. In this technique, the mold (made of quartz, indium tin oxide or hydrogen silsesquioxane) [81–83] is pressed into the UV-curable solution at room temperature after which the solution is photopolymerized by UV-irradiation (Fig. 3c). Due to the low viscosity of the resist, only low pressure is needed to press the mold into the resist. After the detachment of the mold, a replica of the mold's topography remains in the resist layer.

There are some advantages of UV-NIL over thermal NIL: (i) UV curing is rapid, therefore, high-throughput can be achieved; (ii) it can be performed at room temperature and low pressure; (iii) the low viscosity of the polymeric precursors facilitates filling of high aspect ratio cavities; (iv) since thermal cycling is not required in UV-NIL, accurate shape transfer can be obtained. In both cases, a thin residual layer remains, which is typically thinner than found for conventional lithography.

Acrylates are most often used in UV-NIL formulations, because of their commercial availability, low viscosity, and rapid photopolymerization via radical propagation [26]. However, the application of acrylates requires an inert atmosphere since oxygen is a strong radical inhibitor for this process. Vinyl ethers have been proposed to replace acrylates since their polymerization proceeds via a cationic mechanism which is insensitive to oxygen [84]. The limitation of vinyl ether formulations is that they adhere to the substrate more strongly so that double force is required for mold release. This is overcome by the higher tensile strength of vinyl formulations. Fig. 6 shows some UV-curable resists used for imprinting.

Shrinkage is an important parameter to be optimized to avoid rupture of the embossed structures during demolding. During UV curing, acrylic and methacrylic monomers undergo a volume contraction by 3–15% and this facilitates demolding. However, the shrinkage makes pattern design and control difficult. In order to obtain high aspect ratio structures the UV irradiation should be controlled. Excessive UV curing causes excessive shrinkage and brittleness of the resist which also results in cracking and breaking during demolding. Insufficient UV curing leads to low

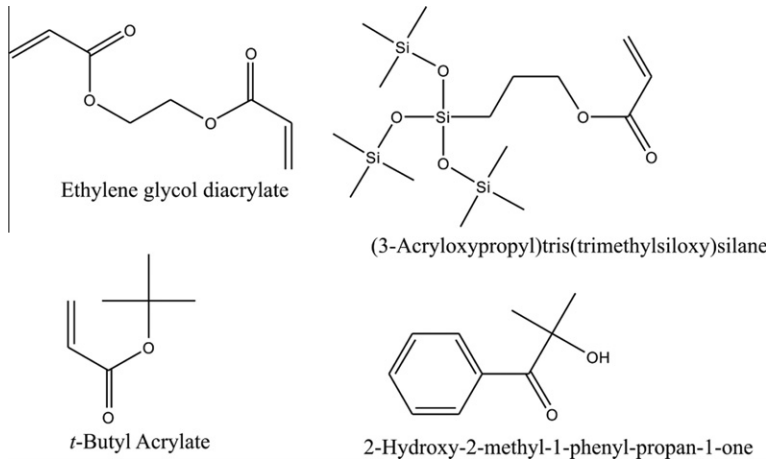

Fig. 6. UV-curable resist components.

cohesive strength of the polymer and causes distortion and collapse of the structures [85]. Profound analyses of factors such as UV polymerization time, vertical walls and surface energy of the mold, surface roughness, and resin transparency affecting replication and demolding during UV-NIL have been reported [85,86].

Jung et al. have developed a UV-NIL process to fabricate 34×34 crossbar circuits with a half-pitch of 50 nm [87]. In this process, a new resist formulation including benzyl methacrylate monomer and irgacure (photoinitiator) was used to overcome the shrinkage problem during curing and to minimize the residual layer thickness. The problem of trapped air during contact with the mold was solved by changing the surface energy of the substrate.

Step-and-flash imprint lithography (SFIL) [88,89], a UV-NIL variant, uses a photocurable prepolymer solution as a material to replicate the topography of a mold. In SFIL, a low viscosity, photocurable liquid or solution is not spin-coated but dispensed in the form of small droplets onto the substrate to fill the voids of the quartz mold. The solution contains a low-molar mass monomer and a photoinitiator. Exposing this solution to UV light cures the photopolymer to make a solidified replica while in contact with the mold. Removing the mold leaves the inverse replica on the substrate. Because of the ability to pattern at room temperature and at low pressure, the template can be stepped to pattern the whole wafer area as in a stepper lithography tool. Examples of imprinted features by SFIL are shown in Fig. 7a–d [90,91].

SFIL avoids incomplete mold filling by using monomeric fluids with a low viscosity. However, complete displacement of the fluid by the mold is prevented by hydrodynamic forces resulting in a residual layer of cured material between patterned features [1,91]. The substrate and the mold should be parallel and flat enough to obtain a uniform residual layer over the entire imprinted area. The residual layer can be removed via etching.

Fluid dynamics is an important issue in the SFIL process [93]. There are several parameters that govern fluid flow of the liquid monomer between the substrate and the template. Parameters governing the fluid flow include the number of initial monomer drops and the relative volume of drops dispensed, flow front arrest at edges of high aspect ratio features and template edges, air entrapment during feature filling, template velocity and force used for imprint, and imprint time.

Pattern density is not a problem for this technique in contrast to thermal NIL [78,94]. The imprint quality for thermal NIL is limited by the differences in pattern size which is not the case for SFIL since a low viscosity fluid is used. However, shrinkage as a result of polymerization must be controlled since this could affect the size, shape and the placement of the replicated structures.

By using an SFIL multilayer method, PMMA lines of 60 nm with an aspect ratio of 6 and 80 nm lines with an aspect ratio of 14 were reported in early publications [36]. Multilayer device fabrication is possible since distortions caused by differential thermal expansion are not an issue. This process can pattern dielectric gates for the fabrication of a metal oxide semiconducter field-effect transistor (MOSFET) and is also being developed to pattern curved surfaces and topographies in a single step. The fabrication of contact holes of 80 nm was demonstrated which is a significant advance in high density semiconducter devices [91].

A bi-layer SFIL process which uses two different materials with two different etch selectivities has been performed to pattern PFS. After patterning of the UV-curable resist, PFS was spin-coated onto the imprinted structures to form bilayer structures and subsequent treatment with argon and oxygen plasma provides patterns of PFS with good reproducibility because of the high etch contrast between the two polymers. The technique allows the possibility of creating etch-resistant patterns of PFS with sizes down to the nanometer range [95].

The ultimate resolution of replication by SFIL is unknown but it has been limited by the size of the structures created on the template. Different methods have been employed to fabricate templates, one of which is the use of EBL which requires several processing steps: application of resist onto a fused silica substrate, electron beam exposure, resist development, oxygen plasma etching, chrome etching, resist stripping and fused silica dry etching [82,88]. In another process, a conductive and transparent layer of indium tin oxide on the glass substrate was incorporated to suppress charging during SEM inspection, and the UV characteristics of the final template were affected minimally which resulted in features as small as 30 nm

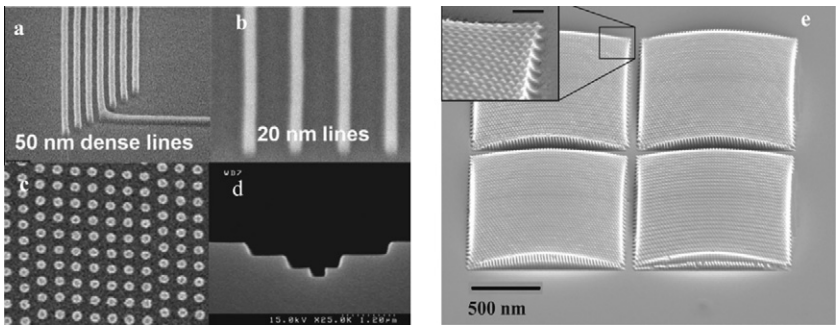

Fig. 7. SEM images of structures imprinted by the S-FIL process: (a) 50 nm dense lines, (b) 20 nm semidense lines, (c) 60 nm posts, and (d) three-tiered structures [90,91]. (e) SEM image of an S-FIL replicated structure (the inset scale bar shows 80 nm lenses on the surface) [92]. Reproduced with permission from [90,92]. Copyright © 2003, 2008 Elsevier B.V. Reproduced with permission from [91]. Copyright © 2005 Elsevier Ltd.

[91]. In another template fabrication process, to eliminate the etching process, a film of hydrogen silsesquioxane (HSQ) was spin-coated on the ITO layer and then directly written with e-beam lithography. The use of HSQ for direct patterning of SFIL template structures is very convenient since it becomes a durable oxide in its cured state [83]. The use of FIB writing as an alternative process to EBL has been demonstrated for the fabrication of 3D structures for SFIL templates which reduces the number of aforementioned lithography steps [92]. As an example, Fig. 7e shows a fabricated array of concave Motheye lenses employing FIB and then replicated through SFIL imprinting.

3.4. Soft lithography

Soft lithography refers to a collection of pattern replication methods that rely on an elastomeric mold [8]. The process can be separated into two parts: fabrication of elastomeric elements by casting and thermal curing of a liquid prepolymer on a master and the use of these elements as a mold or stamp in a subsequent patterning process (Fig. 3d). A number of polymers can be used for molding. Elastomers such as poly(dimethylsiloxane) or PDMS (for example, Sylgard 184, Dow Corning) are a versatile class of polymers for replication of the master [21]. PDMS has a number of useful properties for nanofabrication as it is durable, inert to most of the materials being patterned or molded and chemically resistant to many solvents. Despite the advantages of PDMS, the material also suffers from high compressibility which causes shallow relief features of a stamp to deform, buckle, or collapse. In addition, these relief structures tend to deform upon release from the master because of surface tension [96–99]. Other elastomers such as polyurethane [8], polyimide [8], and cross-linked Novolac resins [100] were reported to be useful as pattern transfer elements. Block copolymer thermoplastic elastomers [101] and polyolefin stamps [102] were investigated and showed superior performance compared to conventional PDMS stamps. A new class of fluoropolymers, perfluoropolyethers (PFPE) [103], was also developed as an alternative to PDMS owing to its excellent release properties and resistance to swelling by organic solvents and monomers. A microfluidic device based on PFPE was fabricated and tested by using different solvents, thus proving its potential in the field of microfluidics [104].

In its most often encountered form, microcontact printing (μCP), a soft lithography technique [105,106], transfers molecules from a patterned PDMS stamp to a substrate by the formation of metal-thiol coordination bonds (Fig. 9) [100,107,108] for the fabrication of self-assembled monolayers (SAMs) of alkanethiols on gold and silver surfaces. In this process, an elastomeric PDMS stamp inked with an appropriate solution of an alkanethiol, is brought into contact with the surface of a substrate to transfer the ink molecules to those regions of the substrate that contact the stamp. The flexibility of the PDMS stamp and the conformal contact between the stamp and the surface of the substrate are both advantageous for printing over large areas and on curved surfaces. The patterned SAMs can be used either as resists in selective wet etching [108] or as templates [109,110] in selective deposition to form patterned structures of a variety of materials: metals, silicon, organic polymers [9,111].

High aspect ratio (HAR) patterns were obtained by direct casting of PDMS onto a mold prepared by using an excimer laser perforating into wax films coated on glass or metal. Micro-hairs of PDMS (post dimensions of 30 μm) were manufactured with aspect ratios of up to 20 (Fig. 8a) [112]. However, thinner size posts obtained were curved in spirals due to capillary effects and air being

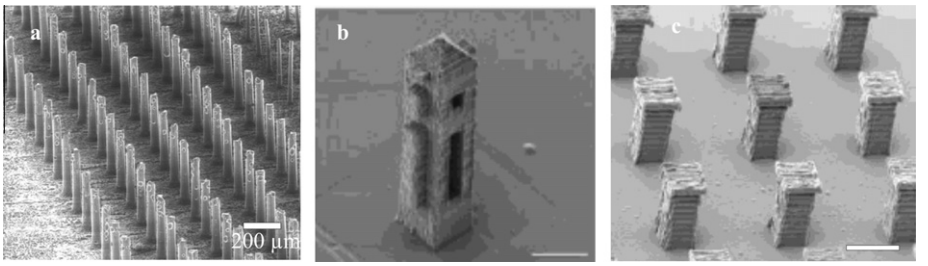

Fig. 8. SEM images of (a) an array of microposts in PDMS [112], (b) and (c) replicas in acrylic resin obtained after soft molding with PDMS (the scale bars in (b) and (c) represent 10 μm) [118]. Reproduced with permission from [112]. Copyright © 2005 IOP Science. Reproduced with permission from [118]. Copyright © 2004 American Chemical Society.

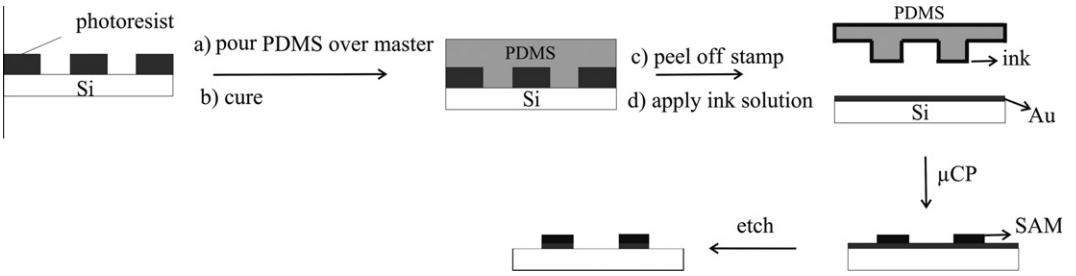

Fig. 9. Schematic illustration of the μCP procedure.

trapped in the holes. X-ray LIGA (a German acronym for lithography, electroplating, and molding) molds have also been used to fabricate HAR structures from PDMS with an aspect ratio of 15 [113]. The low Young's modulus of PDMS limits its use in HAR patterning of submicrometer structures. Soft elastomeric features are affected by gravity, adhesion, and capillary forces and may collapse, generating defects in the pattern formed [9]. To improve the mechanical stability of elastomeric stamps, alternative materials have been proposed such as composite PDMS [114], UV-curable PDMS [115] and photocurable fluorinated organic–inorganic hybrids [116].

Soft molding includes the patterning techniques based on flexible PDMS stamps and has some advantages over molding with hard masters. The demolding step is facilitated by the elasticity and low surface energy of PDMS which also gives the possibility to replicate the size and shape of the features present on the mold by mechanical deformation. Multiple PDMS molds can be inexpensively fabricated from a single master [117].

Various molding processes are available depending on the material to be molded by PDMS and the hardening mechanism. One of these is solvent-assisted micro-molding where the polymer solution is drawn into the cavities of the PDMS mold by capillary forces (Fig. 3e). The others are mainly UV molding of polymer films and micromolding in capillaries (MIMIC) [1,117].

Soft lithography is relatively cheap and flexible and allows one to control surface chemistry which can be modified by plasma treatment and reaction with organosilanes. This makes the technique very useful when complex organic functional groups are needed in chemistry, biology or biochemistry. Replication of 3D structures is possible because of the softness and elasticity of PDMS. Structures created with an acrylic polymer using multiphoton absorption polymerization (MAP) were replicated by microtransfer molding using a PDMS stamp (Fig. 8b and c). It is not possible to use microtransfer molding to replicate every structure generated by the MAP technique but careful study of the effects of peeling rate and angle of PDMS stamp removal could presumably increase the range of structures that can be replicated reproducibly [118].

3.5. Colloidal lithography

Colloidal lithography uses particles which are an attractive tool for nanofabrication due to their ability to self-organize. The self-assembled particles have been used in the fabrication of nanopatterns and lithographic masks. Colloidal lithography is inexpensive, inherently parallel, high-throughput, and has a high materials versatility. It is capable of producing well-ordered, 2D–3D periodic arrays of nanoparticles from a variety of materials on many substrates. Three dimensional layers are of interest for photonic applications, whereas two-dimensional layers are used as etch or lithographic masks [119].

3.5.1. Synthetic methods to prepare colloidal particles

Even though a broad range of colloidal particles is now available commercially, it may still be necessary to produce colloidal particles of desired sizes and compositions. Various polymerization methods such as emulsion, dispersion, precipitation and suspension polymerization can be used to synthesize polymer colloidal particles [120]. Polymer particles such as PS and PMMA are commonly synthesized by emulsion and dispersion polymerization. The particle sizes vary in the range of 0.05–10 μm depending on the reaction conditions. For emulsifier-free emulsion polymerization [121], the reaction temperature and the monomer concentration are the most important factors that control the size of the particles. Increase of the temperature and a decrease of the monomer concentration give rise to a decrease of the particle size since the solubility of the monomer in the aqueous phase depends on the temperature, and the depletion time of the monomer varies with the monomer concentration. The seed polymerization method [122] can be used for monodisperse polymeric spheres larger than 1 μm in diameter. Larger polymer particles are produced by additional repeated polymerization onto the seed polymer latexes which broadens the polydispersity due to the repeated addition of the raw materials. A single-step dispersion polymerization is generally used as an alternative to produce larger particles. In dispersion polymerization, the reaction site is a monomer droplet stabilized by a smaller amount of surfactants and an initiator, which is soluble in oil and diffuses to the monomer droplets which act as a bulk polymerization reactor [119,123].

Stöber et al. [123] developed a technique to prepare inorganic oxide particles, for example silica particles, by using sol–gel chemistry. It is based on the hydrolysis and condensation of tetraethylorthosilicate (TEOS) in a mixture of alcohol, water and ammonia. Synthesis of inorganic particles is achieved following two steps which are nucleation and subsequent growth. To obtain monodisperse particles, these two steps should be separated such that the nuclei can be homogeneously generated without simultaneous growth. In general, the size and polydispersity of particles are related to many factors such as pH, the concentration of the catalyst, the composition of reagents, the type of solvent, and the reaction temperature, which all affect the rates of hydrolysis and condensation [124].

The principles involved in the preparation of particles have been described [125] and it is now possible to obtain uniform metal oxides, halides, sulfides, selenides, phosphates, carbonates, etc. in different morphologies. Properties of these powders can be modified either by producing solids of internally mixed composition or by coating cores with shells of a different compound [125].

3.5.2. Methods of colloidal crystal assembly

Dispersion stability and the crystallization of the colloidal dispersion are governed by interactions including Van der Waals forces, steric repulsion, and Coulombic repulsion. During the fabrication of colloidal templates or masks, the evaporation of solvent may induce self-assembly of the colloidal particles which makes capillary forces important in the arrangement of the particles [119,126]. Fig. 10 shows the strategies for fabricating 2D colloidal arrays including dip-coating, floating on an interface, electrophoretic deposition, physical and chemical template-guided self-assembly, and spin-casting.

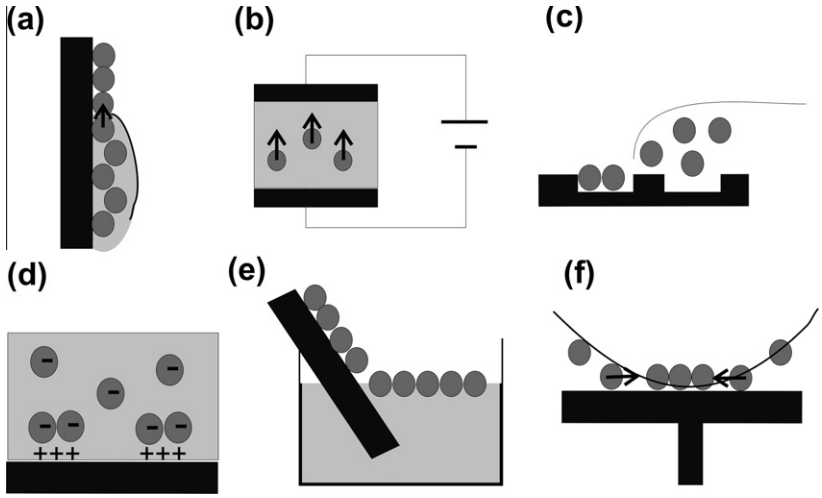

Fig. 10. Self-assembly strategies to create ordered colloidal arrays: (a) dip-coating, (b) electrophoretic deposition of colloids, (c) template-guided self-organization, (d) chemical or electrochemical self-organization of colloidal particles, (e) lifting up a colloidal array from an interface using a substrate, (f) spin-coating of assembled colloidal particles. Reproduced with permission from [119]. Copyright © 2006 WILEY-VCH Verlag GmbH.

In dip-coating [127], capillary forces and controlled evaporation induce self-organization of particles (Fig. 10a). The quality of the self-organization is determined by the evaporation rate, which can be controlled by a step motor which helps to lift up the substrate from the colloidal suspension at a controlled rate such that the entire surface can be covered by domains.

Electrophoretic deposition [128,129] of the particles employs electric fields to move the particles as shown in Fig. 10b. Particle assembly takes place inside a thin layer of a colloidal suspension sandwiched between conducting substrates such as indium tin oxide coated glass substrates followed by applying the electric field across the electrodes [40]. Electrophoretic movement not only accelerates the sedimentation speed of small colloidal particles but also guides the growth of a colloidal crystal over a large area in a controlled manner. Important prerequisites for successful electrophoretic particle deposition are that the particles possess an appreciable magnitude of surface charge to form stable suspensions and to insure a sufficient electrophoretic mobility [130]. The combination of patterned electrode templates with electric field driven assembly was shown to provide control over crystal packing and lattice orientation. Hexagonal and square type packing symmetries of 2D colloidal monolayers were obtained over large surfaces by using this so called graphoepitaxy method [129].

Defect formation can be suppressed by template-assisted self-assembly of colloidal particles [131]. A chemically [132,133] (Fig. 10d) or topographically [134] (Fig. 10c) patterned substrate can be used for the selective deposition of colloidal particles. Physical templates based on relief structures patterned on the surfaces of solid substrates have been used by Xia et al. to produce a variety of structures including polygonal, polyhedral, spiral, and hybrid aggregates of spherical particles that are difficult to fabricate with other methods [134]. The structure of the aggregates was controlled by changing the shape and the dimensions of the template using conventional photolithography, which also prevented the production of templates with feature sizes smaller than 100 nm.

Fig. 10e shows the assembly of a colloidal array floating on an interface. The quality and packing of the array at the interface can be controlled by changing the concentration of the particles or electrolytes, the particle size, the surface charge and the hydrophobicity of the particles [135,136]. For example, silica colloids modified by silanizing the surface to enhance the hydrophobicity were self-assembled at an octane/water interface. A monolayer without variation in the layer thickness could be obtained, which is not possible for evaporation-induced self-assembly [137]. The Langmuir–Blodgett film technique can also be used to obtain such a uniform layer [138].

Another way of preparing a colloidal array is by using spin-coating [139]. The colloidal particles organize themselves into a hexagonal array more rapidly due to the centrifugal forces (Fig. 10f). The thickness of the particle layer is controlled by adjusting the particle loading and the spin speed. Spin-coating provides advantages for both scaling up and mass production since the process is rapid and compatible with wafer processing.

3.5.3. Nanopatterning with colloidal masks

Colloidal particles in a hexagonally packed array can be used as a mask so that deposition or etching proceeds through the interstices between the colloidal particles. Evaporation and sputtering into these interstices has been used to produce very thin films (<30 nm) of metals and inorganic oxides. The sputtered material can be chosen without any limitation, and the size, height, and number density of the metal dots can be controlled by simply adjusting the particle size and the sputtering conditions.

The use of colloidal particle arrays as masks for metal sputtering or for etching substrates was pioneered by Deckman et al. and Fischer et al. [140,141]. Duyne et al. [142] used single- or double-layered PS particles on

various substrates as a mask for metal deposition as illustrated in Fig. 11. As seen in Fig. 11a and b, a hexagonally ordered triangular array of metal dots formed from a single layer colloidal mask, and a spherical dot array with different unit lattices was fabricated from the double-layer mask (Fig. 11c and d). The reason for the formation of a spherical dot array is that when a second layer of nanospheres assembles onto the first, every other threefold hole is blocked, and a smaller density of sixfold interstices results as shown in Fig. 11c and d.

Colloidal arrays as masks have also been used for the nanofabrication of various organic and inorganic materials. The deposited materials, in some cases, can be used as seeds for the growth of other functional materials. For instance, carbon nanotubes were grown on nickel nanodots that were pre-deposited through a colloidal mask by using plasma-enhanced chemical vapor deposition (PECVD) (Fig. 12a) [143]. Zinc oxide nanorod arrays were also prepared using PS particles as a template for patterning gold catalyst particles and subsequent bottom-up growth in a tube furnace using chemical vapor deposition (Fig. 12b) [144]. Similarly, an organic light-emiting nanodiode (OLED) array was fabricated by deposition of multilayers through the interstices of the particle array. This method does not cause any etching damage, as is sometimes encountered with conventional masking processes [145]. Patterning of ferromagnetic arrays was demonstrated over an area greater than 1 cm^2 without agglomeration of particles after metal evaporation which gave control over the diameter, aspect ratio, and pitch of the fabricated elements.

Sputtered metal arrays can be used as etching masks to create surface topography. Silicon nanopillars with diameters as small as 40 nm and aspect ratios of up to 7 were fabricated by preparing an aluminum etch mask using a PS particle array (Fig. 12c) [146]. Large-area periodic silicon nanopillar arrays have been obtained after metal deposition, lift-off, and etching processes. By varying the etching parameters, such as mask materials and etching recipes, the size and the shape of silicon nanopillars can be modified, thus size and shape control of nanostructures can be achieved [146].

The combination of colloidal lithography (CL) and alkanethiol self-assembly was used to create substrates with controlled surface topography and chemical composi-

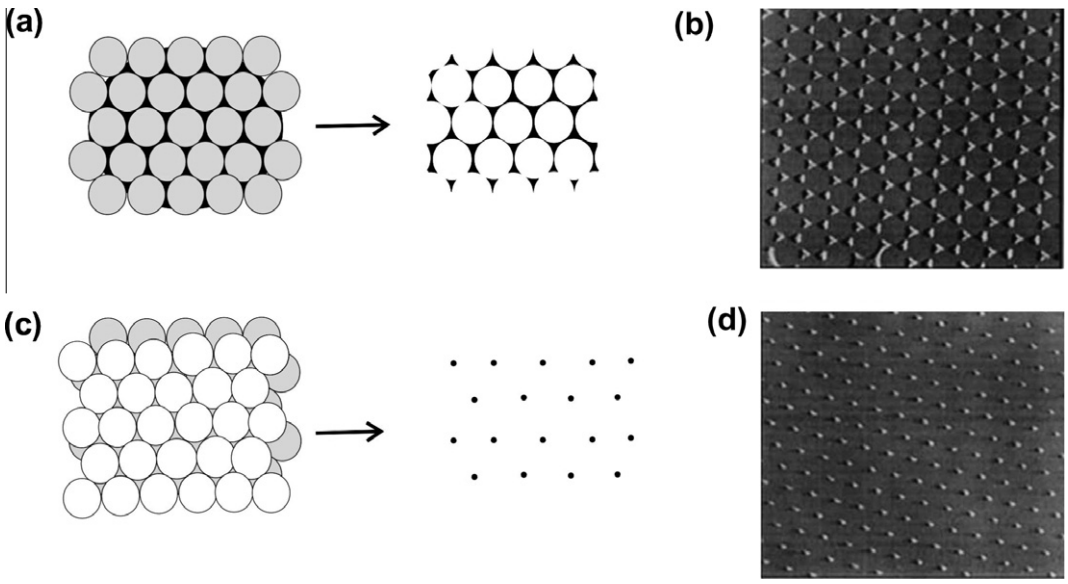

Fig. 11. (a) Schematic diagram of a single layer nanosphere mask and (b) a hexagonally ordered triangular array of metal dots after removal of the template. (c) Schematic diagram of a double layer nanosphere mask and (d) spherical dot arrays after removal of the template. Reproduced with permission from [142]. Copyright © 1995 American Vacuum Society.

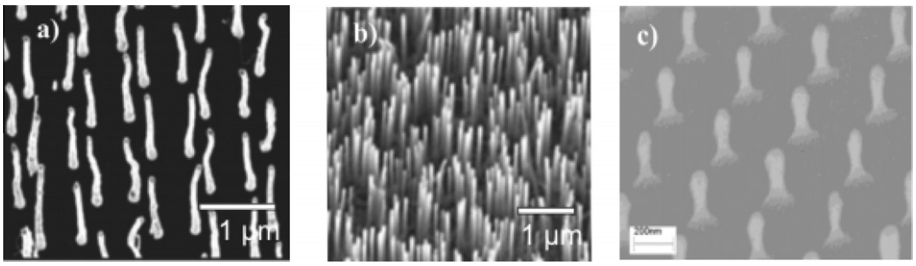

Fig. 12. (a) Vertically aligned carbon nanotube array by using plasma-enhanced chemical vapor deposition (PECVD) [143]. (b) ZnO nanorod arrays prepared using gold catalyst particles and subsequent bottom-up growth in a tube furnace using chemical vapor deposition [144]. (c) SEM image of silicon nanopillars fabricated by means of an aluminum etch mask obtained using a PS particle array [146]. The scale bar indicates 200 nm. Reproduced with permission from [143,144,146]. Copyright © 2003, 2004, 2003 American Chemical Society.

tion. Patterns exhibiting also chemical contrast allow one to investigate the interfacial interactions or adsorption behavior of biomolecules and nanoparticles. For example, Michel et al. created topographical contrast via colloidal patterning to design platforms for the attachment of targeted proteins [147]. Nanopillars of TiO_2 (50–90 nm in diameter, 20 nm in height) on oxidized silicon were fabricated by using colloidal lithography and were then rendered hydrophobic by the selective self-assembly of an organophosphate, whereas a poly(ethylene glycol)-grafted copolymer was adsorbed onto the surrounding SiO_2, rendering it protein resistant. Further binding of streptavidin onto the organophosphate and immobilization of biotinylated liposomes to the streptavidin was accomplished successfully [147].

Tan et al. [148] used particle arrays as a mask to fabricate a dome structure by reactive ion etching [40] which converts the spheres into nonspherical particles. Single and double layers of packed colloidal polystyrene microspheres of uniform size (diameter 1.2 μm) were spin-coated onto cleaned Si substrates, which were then exposed to CF_4 and O_2 plasma mixtures. Due to preferential etching in the direction normal to the surface of the substrate, the microspheres were reduced to a nonspherical form resembling a biconvex microlense.

Spherical colloidal particles can be utilized for preparing various types of porous materials that exhibit precisely controlled pore sizes and highly ordered 3D porous structures. After drying the colloidal array, the voids between the colloidal spheres are fully infiltrated with a liquid precursor such as an ultraviolet [19] or thermally curable organic prepolymer [125], or an ordinary organic monomer (plus an initiator) [149]. Subsequent solidification of the precursor and removal of the colloidal spheres gives a 3D porous structure. Johnson et al. [149] prepared ordered mesoporous polymers by filling the pores in the colloidal crystals (silica spheres of 35 nm in diameter) with divinylbenzene (DVB), ethyleneglycol dimethacrylate (EDMA), or a mixture of the two. Polymerization and subsequent dissolution of the silica template left a polycrystalline network of interconnected pores. When mixtures of DVB and EDMA were used, the pore size of the polymer replicas varied continuously between 35 and 15 nm because the polymer shrinks when the silica template is removed [149]. Initiated chemical vapor deposition (iCVD) has also been used to produce grafted polymeric layers (Fig. 13) [150]. Patterns were generated for a broad range of materials including organic polymers (pBA, pHEMA), fluoropolymers (pPFDA, pPFM) and organosilicones. Since iCVD is a solvent-free process, it has many advantages compared to solution polymerization [150].

In an another study, a new approach for fabricating porous structures on silicon substrates and on polymer surfaces, using colloidal particle arrays with a polymer mask of PFS, has been demonstrated [151]. Silica nanoparticles of different sizes were used as starting materials and PFS as an etch-resistant polymer to produce a negative replica of the nanoparticle array. The combination of techniques used in this process allows the fabrication of uniform, nanoporous, free standing PES membranes, which were further employed for filtration experiments.

3.5.4. Modification of colloidal masks

One of the disadvantages of the CL method is the limited control over the shape of the patterns, which is triangular or spherical. Adjustment of the deposition method and modification of the colloidal masks have been suggested to overcome this limitation [119]. The deposition method can be modified by tilted or rotated deposition through the as prepared colloidal mask. The angle between the deposition flow and the substrate normal can be controlled and a variety of structures (elongated triangles or double triangles) has been obtained by varying this angle. However, the shapes obtained are restricted by the mask shape [119].

A more effective approach is to modify the colloidal particles by suitable post-treatment such as RIE, ion milling, or annealing. The deformation of polymeric beads such as PS and PMMA occurs above the glass transition temparature and this has been utilized to modify the colloidal mask for fabricating a gold disk array via CL. The size of the disk was adjusted by changing the annealing time, since polymeric particles spread over a wider distance with the annealing time (Fig. 14a–f). Microwave heating can also be used to anneal the polymer particles which gives more precise control over the degree of annealing [152]. Kosiorek et al. produced particles with morphologies such as rings, rods, and dots by changing the mask morphology by temperature processing and varying the evaporation conditions [152]. The technique was shown to scale down the size of metallic nanoparticles from 200 to 30 nm, while preserving the original nanosphere spacing and order. It was shown that by temperature treatment it is easy to control the spaces between the spheres, and therefore the size of the particles deposited through the PS mask.

Meanwhile, RIE has been used to modify the colloidal mask by changing the size and the shape of the particles [153]. RIE has been employed to control the surface morphology and roughness and to enhance the surface hydrophilicity in polymeric and biological applications. RIE was used to fabricate polymeric nanofibrillar surfaces and patterned structures using colloidal single layers and double layers. Choi et al. have created well organized layers of nonspherical colloidal particles by using anisotropic RIE of the spherical polymer latexes that were stacked layer-by-layer, with the top layer acting as a mask [154]. The

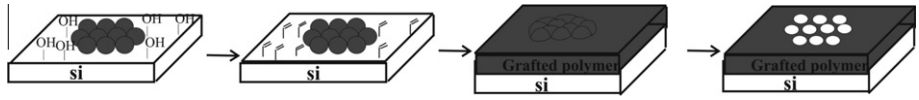

Fig. 13. Schematic process for producing polymeric nanostructures using CL. A hydroxylated substrate was treated with a vapor-phase silane coupling agent, which covalently attaches the vinyl groups to the substrate in the exposed regions of the colloidal mask. The polymer was grafted and the grafted film was sonicated to remove the colloidal template, leaving an array of bowl-shaped nanostructures. Reproduced with permission from [150]. Copyright © 2009 American Chemical Society.

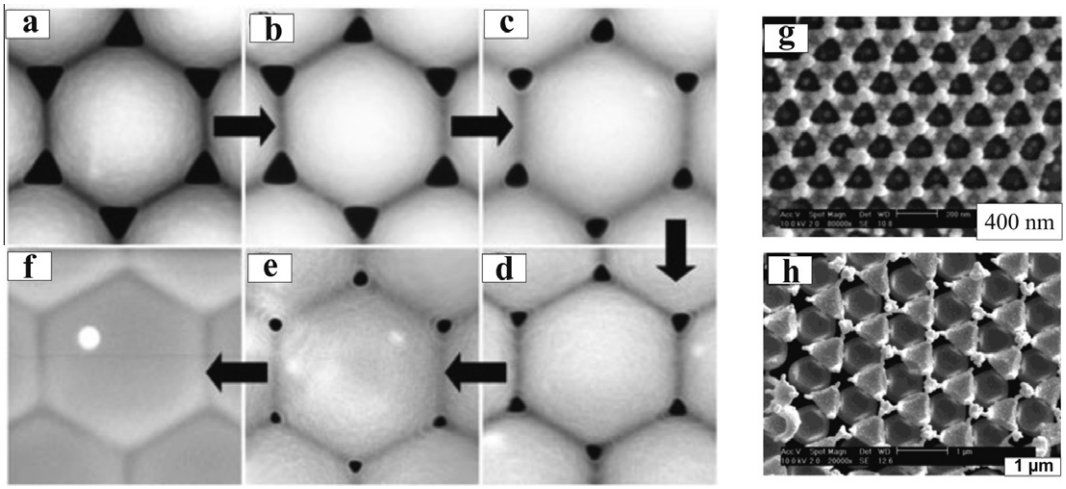

Fig. 14. A 540-nm PS latex mask annealed in 25 mL of a water/EtOH/ acetone mixture by (a) 1, (b) 2, (c) 4, (d) 6, (e) 7, and (f) 10 microwave pulses. Reproduced with permission from [152]. Copyright © 2005 WILEY-VCH Verlag GmbH. (g) Binary particle arrays and 2-D nanopatterns produced from a double layer of small PS beads (200 nm). (h) Ternary particle arrays produced after partial RIE etching of PS beads in fcc symmetry. Reproduced with permission from [154]. Copyright © 2004 American Chemical Society.

shadowing effect from the upper layer of particles to the layers beneath resulted in nonspherically etched polymeric structures (Fig. 14g). The resulting patterns and particle shapes were dependent on the crystal orientation relative to the substrate (Fig. 14h), the number of colloidal layers, and the RIE conditions.

4. Pros and cons of the presented techniques and future prospects

Currently, photolithography is the most widely used technique in microelectronics due to its several advantages, such as full wafer processing and short exposure time (in the range of several seconds), implying a fast process. On the other hand, the main drawbacks of this technique are the limited resolution and the limited possibilities of working with pre-existing topography or curved substrates [1,2]. A number of novel approaches to increase the resolution of the technique [155] have been developed but these result in increased operational costs. Extreme Ultraviolet Lithography (EUV) constitutes a highly promising development. EUV is an emerging technology, originally proposed in 1988, but its implementation has been postponed several times. At present, the 193 nm lithography constitutes the state of the art. Shorter wavelength lithography, or next generation lithography (NGL) uses shorter wavelength ultraviolet light (157 nm), EUV light (120–10 nm), X-ray (0.4 nm) and also includes electron and ion beam lithography [156]. As the 157 nm lithography is being abandoned, technologies based on 193 nm wavelengths will in time be replaced by technologies developed around 13.5 nm wavelengths, which necessitates major revisions in EUV resist technology, EUV aligners or printers, EUV masks, etc. Polymer resists are actively being developed for use in EUV lithography. High T_g polycarbonates are one promising class of materials for use as resists, as they possess a sufficient sensitivity to EUV irradiation [157]. Other requirements are a high etch resistance to enable pattern transfer into silicon wafers. Patterning with EUV lithography has been demonstrated and features with critical dimensions below 30 nm at a half pitch of 50 nm were achieved. With further developments in polymer resist formulation and developer within sight, much can be expected from this lithography technology.

Fabrication of smaller scale patterns can be achieved by scanning beam lithographic techniques, such as electron beam and focused ion beam lithography. Electron beam lithography uses an electron beam to write in electron sensitive resists, and is widely used as a serial process. The diffraction effect is no longer a limiting factor for the resolution since the wavelength is much lower for electrons than that of photons with the same energy. The dose and the size of the beam have to be optimized by using high or low energy electron beams to minimize proximity effects that occur when the effective exposed area is larger than the beam size. The need for vacuum for operation and long processing time increase the cost of this technique.

Therefore, new methods which circumvent limitations due to either diffraction or high cost have emerged and are known as unconventional lithography e.g. molding, embossing, and printing. Unconventional nanofabrication techniques offer alternatives to photolithography and create opportunities for fabrication on nonplanar surfaces and over large areas. Among the lithography techniques, both thermal NIL and UV-NIL can offer several advantages such as nanometer-scale resolution and high througput with a low process cost. A stamp fabricated by EBL can be reused several times. In a thermal NIL process, since the resist is deformed by increasing the temperature and pressure, the throughput of the imprint process is limited and the lifetime of the imprint template is shortened. Moreover, thermal cycling causes problems in the stability and fidelity of the pattern transfer. The removal of the residual layer is another issue. Resists should possess a sufficiently high etch resistance but residual resist layers must be removable, for instance by exposure to RIE. This led to new

generations of polymers with improved etch resistivity for thermal NIL. UV-NIL has some advantages over thermal NIL as being rapid and operational at room temperature with low pressure. UV-NIL does not require temperature cycling, leading to higher throughput than in thermal NIL, and the transparency of the template offers the possibility for convenient optical and high-precision alignment. UV-NIL uses a low-viscosity resist which also beneficially influences the imprint force and compression time. On the other hand, one of the difficulties is that the resolution is restricted by the mold pattern that is expensive to fabricate.

Recent work has shown further advancement in NIL resolution. Nanoimprint molds were fabricated using an electron-beam lithography process with a hydrogen silsesquioxane (HSQ) resist on silicon substrates. The HSQ patterns were directly used for nanoimprint or transferred into the underlying substrate to increase the aspect ratio of the patterns prior to imprint. The method could be used to create sub-10 nm feature sizes and sub-15 nm half-pitch arbitrary patterns in functional materials [158]. Novel developments in the nanoimprint process include wafer bowing, which allows the imprint force to be applied uniformly and systematically from center to edge, preventing air from being trapped. In this scheme the mechanical path between mold and wafer is shortened, which helps to preserve alignment during mold-wafer approach. Using the concept of wafer bowing, excellent overlay and resolution (<10 nm) were achieved [159]. These important developments increase the viability of nanoimprint lithography for manufacturing semiconductor devices [160,161].

Other unconventional lithography techniques such as soft lithography and nanosphere lithography have their own advantages and disadvantages. Soft lithography is an unconventional technique which can be applied to nonplanar surfaces, and allows the patterning of a range of materials. The material used for stamping is made of PDMS, which renders the process inexpensive. The use of an elastomeric mold rather than a rigid mold allows it to conform to nonplanarity in surface topography. Swelling of the mold, on the other hand, can cause distortion of the features. These issues have been addressed and the microcontact printing technique has seen spectacular improvements since its discovery by Whitesides and coworkers in 1993. A broad range of stamp materials has become available, allowing the use of a variety of polar and non-polar inks which in turn increased the applicability of the technique. Printing resolution has been improved significantly by developments in stamp materials and by the use of nondiffusive inks, which led to achievable resolutions in the sub-100 nm range. Along with various approaches aimed at minimizing ink spreading, such as replacing liquid inks by polymers, methods were developed that avoid the use of inks completely and instead rely on a catalytic reaction between the stamp and substrate [162]. An example of a highly successful, inkless printing approach is the use of a rigid, polyurethane-polyacrylate stamp capable of supporting high-resolution patterns, to which a chemical catalyst is bound covalently [163]. These exciting developments underscore the huge potential of the microcontact printing technique in all its variations for creating chemical, supramolecular and biomolecular patterns on hard and flexible surfaces in a highly cost-effective way. Interestingly, microcontact printing can also be carried out with a cylindrical rolling stamp, in principle allowing the automated large area patterning of substrates with submicrometer features [164,165].

Nanosphere lithography (NSL) employs self-assembled single or double layers of particles as lithographic masks or templates to produce nanosized features of polymers and metals in a low cost and simple manner [166–168]. Complex equipment is not required to create patterns on the nanometer scale and the assembly of the particles is achieved readily by spin-coating or dip-coating. However, most studies on colloidal materials have been limited to spherical particles. A variety of methods have been developed to obtain non-spherical colloids, but few of them could generate monodispersed features. The formation of defects during colloidal assembly is another problem of the technique.

Novel polymeric resist materials, combined with selective structuring methodologies, enable the fabrication of patterns with ever smaller feature sizes. Highly promising approaches include probe-based nanolithography methods involving the local removal of resist polymer using atomic force microscopy (AFM) heated tips. Tip-based patterning methods such as local anodic oxidation, field-induced deposition of materials and the tip-induced modification or removal of thermomechanically responsive organic materials are established. The serial nature of tip-based patterning processes limits their efficiency, however, this issue has been overcome using multi-probe lithography techniques. A breakthrough in patterning efficiency was recently realized by employing self-amplified depolymerization polymers (SAD) as resists in probe-based nanolithography. Here, the thermally induced breaking of a single bond leads to spontaneous depolymerization of the entire chain. Using polyphthalaldehyde SAD polymers, two-dimensional nanoscale patterns could be written with high efficieny. Also, arbitrary three-dimensional patterns were created with about 40 nm lateral and 1 nm vertical resolution. The employed SAD polymer also possessed a high reactive ion etch resistance, allowing a direct pattern transfer into silicon substrates [169,170]. The nm-precise fabrication of three-dimensional structures is highly valuable for creating e.g. nanoimprint lithography templates.

5. Conclusions

Conventional and unconvential techniques have enabled fabrication of 2D and 3D structures ranging from several tens of nanometers to micrometer scales. Historically, photolithography has been the dominant technique for replication despite its resolution limit. Photolithography continues to overcome obstacles to achieve new resolution limits which, however, increases the cost. The high cost of conventional equipment for nanofabrication paves the way for unconventional techniques. Unconventinal techniques for nanofabrication are being widely accepted and they are extensively explored for research purposes. Molding, embossing, and printing techniques provide

higher resolution patterning with high througput at a lower cost. Despite all recent progress in patterning, each patterning method has its own specific strengths and advantages and cannot meet the requirements of all fabrication needs. In addition, the large-scale fabrication of surface patterns by using the reported methods still remains a big challenge. Combining different fabrication methods could help the future development of devices and their performances.

References

[1] Gates BD, Xu QB, Stewart M, Ryan D, Willson CG, Whitesides GM. New approaches to nanofabrication: molding, printing, and other techniques. Chem Rev 2005;105:1171–96.
[2] Ito T, Okazaki S. Pushing the limits of lithography. Nature 2000;406:1027–31.
[3] Wallraff GM, Hinsberg WD. Lithographic imaging techniques for the formation of nanoscopic features. Chem Rev 1999;99:1801–21.
[4] Gamo K. Nanofabrication by FIB. Microelectron Eng 1996;32:159–71.
[5] Xia YN, Kim E, Zhao XM, Rogers JA, Prentiss M, Whitesides GM. Complex optical surfaces formed by replica molding against elastomeric masters. Science 1996;273:347–9.
[6] Chou SY, Schablitsky SJ, Zhuang L. Application of amorphous silicon subwavelength gratings in polarization switching vertical-cavity surface-emitting lasers. J Vac Sci Technol B 1997;15:2864–7.
[7] Chou SY, Krauss PR, Renstrom PJ. Imprint lithography with 25-nanometer resolution. Science 1996;272:85–7.
[8] Xia YN, Whitesides GM. Soft lithography. Angew Chem Int Ed 1998;37:551–75.
[9] Xia YN, Whitesides GM. Soft lithography. Annu Rev Mater Sci 1998;28:153–84.
[10] Eigler DM, Schweizer EK. Positioning single atoms with a scanning tunneling microscope. Nature 1990;344:524–6.
[11] Piner RD, Zhu J, Xu F, Hong SH, Mirkin CA. "Dip-pen" nanolithography. Science 1999;283:661–3.
[12] Wouters D, Schubert US. Nanolithography and nanochemistry: probe-related patterning techniques and chemical modification for nanometer-sized devices. Angew Chem Int Ed 2004;43:2480–95.
[13] Rogers JA, Paul KE, Jackman RJ, Whitesides GM. Using an elastomeric phase mask for sub-100 nm photolithography in the optical near field. Appl Phys Lett 1997;70:2658–60.
[14] Rogers JA, Paul KE, Jackman RJ, Whitesides GM. Generating similar to 90 nanometer features using near-field contact-mode photolithography with an elastomeric phase mask. J Vac Sci Technol B 1998;16:59–68.
[15] Melosh NA, Boukai A, Diana F, Gerardot B, Badolato A, Petroff PM, et al. Ultrahigh-density nanowire lattices and circuits. Science 2003;300:112–5.
[16] Xu QB, Gates BD, Whitesides GM. Fabrication of metal structures with nanometer-scale lateral dimensions by sectioning using a microtome. J Am Chem Soc 2004;126:1332–3.
[17] Whitesides GM, Laibinis PE. Wet chemical approaches to the characterization of organic-surfaces - self-assembled monolayers, wetting, and the physical organic-chemistry of the solid liquid interface. Langmuir 1990;6:87–96.
[18] Whitesides GM, Mathias JP, Seto CT. Molecular self-assembly and nanochemistry: a chemical strategy for the synthesis of nanostructures. Science 1991;254:1312–9.
[19] Haisma J, Verheijen M. Van den Heuvel K, van den Berg J. Mold-assisted nanolithography: a process for reliable pattern replication. J Vac Sci Technol B 1996;14:4124–8.
[20] Chou SY, Krauss PR, Renstrom PJ. Imprint of sub-25 nm vias and trenches in polymers. Appl Phys Lett 1995;67:3114–6.
[21] Rogers JA, Nuzzo RG. Recent progress in soft lithography. Mater. Today 2005;8:50–6.
[22] Moreau WM. Semiconductor lithography: principles and materials. New York: Plenum; 1988.
[23] Rothschild M, Bloomstein TM, Kunz RR, Liberman V, Switkes M, Palmacci ST, et al. Liquid immersion lithography: why, how, and when? J Vac Sci Technol B 2004;22:2877–81.
[24] Rothschild M. Projection optical lithography. Mater Today 2005;8:18–24.
[25] Sanders DP. Advances in patterning materials for 193 nm immersion lithography. Chem Rev 2010;110:321–60.
[26] del Campo A, Arzt E. Fabrication approaches for generating complex micro- and nanopatterns on polymeric surfaces. Chem Rev 2008;108:911–45.
[27] Han M, Lee W, Lee SK, Lee SS. 3D microfabrication with inclined/rotated UV lithography. Sens Actuators A Phys 2004;111:14–20.
[28] Sato H, Houshi Y, Shoji S. Three-dimensional micro-structures consisting of high aspect ratio inclined micro-pillars fabricated by simple photolithography. Microsys Technol 2004;10:440–3.
[29] Romanato F, Tormen M, Businaro L, Vaccari L, Stomeo T, Passaseo A, et al. X-ray lithography for 3D microfluidic applications. Microelectron Eng 2004;73–4:870–5.
[30] Yang H, Jin A, Luo Q, Gu C, Cui Z. Comparative study of e-beam resist processes at different development temperature. Microelectron Eng 2007;84:1109–12.
[31] Czaplewski DA, Tallant DR, Patrizi GA, Wendt JR, Montoya B. Improved etch resistance of ZEP 520A in reactive ion etching through heat and ultraviolet light treatment. J Vac Sci Technol B 2009;27:581–4.
[32] Elsner H, Meyer HG. Nanometer and high aspect ratio patterning by electron beam lithography using a simple DUV negative tone resist. Microelectron Eng 2001;57–8:291–6.
[33] Xia YN, Rogers JA, Paul KE, Whitesides GM. Unconventional methods for fabricating and patterning nanostructures. Chem Rev 1999;99:1823–48.
[34] van Kan JA, Bettiol AA, Watt F. Three-dimensional nanolithography using proton beam writing. Appl Phys Lett 2003;83:1629–31.
[35] Okazaki S. Resolution limits of optical lithography. J Vac Sci Technol B 1991;9:2829–33.
[36] Colburn M, Grot A, Choi BJ, Amistoso M, Bailey T, Sreenivasan SV, et al. Patterning nonflat substrates with a low pressure, room temperature, imprint lithography process. J Vac Sci Technol B 2001;19:2162–72.
[37] Junarsa I, Nealeya PF. Fabrication of masters for nanoimprint, step and flash, and soft lithography using hydrogen silsesquioxane and x-ray lithography. J Vac Sci Technol B 2004;22:2685–90.
[38] Ansari K, Shao PG, van Kan JA, Bettiol AA, Watt F. Proton beam fabrication of nickel stamps for nanoimprint lithography. Nucl Instrum Methods Phys Res Sect B 2005;231:407–12.
[39] Chou SY, Krauss PR, Renstrom PJ. Nanoimprint lithography. J Vac Sci Technol B 1996;14:4129–33.
[40] Larsen AE, Grier DG. Melting of metastable crystallites in charge-stabilized colloidal suspensions. Phys Rev Lett 1996;76:3862–5.
[41] Maximov I, Sarwe EL, Beck M, Deppert K, Graczyk M, Magnusson MH, et al. Fabrication of Si-based nanoimprint stamps with sub-20 nm features. Microelectron Eng 2002;61–2:449–54.
[42] Sotomayor Torres CM, Zankovych S, Seekamp J, Kam AP, Clavijo Cedeño C, Hoffmann T, et al. Nanoimprint lithography: an alternative nanofabrication approach. Mater Sci Eng C 2003;23:23–31.
[43] Taniguchi J, Tokano Y, Miyamoto I, Komuro M, Hiroshima H. Diamond nanoimprint lithography. Nanotechnology 2002;13:592–6.
[44] Li MT. PhD thesis. Princeton University; 2003.
[45] Taniguchi J, Koga K, Kogo Y, Miyamoto I. Rapid and three-dimensional nanoimprint template fabrication technology using focused ion beam lithography. Microelectron Eng 2006;83:940–3.
[46] Katoh T, Nishi N, Fukagawa M, Ueno H, Sugiyama S. Direct writing for three-dimensional microfabrication using synchrotron radiation etching. Sens Actuators A: Phys 2001;89:10–5.
[47] Jaszewski RW, Schift H, Gröning P, Margaritondo G. Properties of thin anti-adhesive films used for the replication of microstructures in polymers. Microelectron Eng 1997;35:381–4.
[48] Keil M, Beck M, Frennesson G, Theander E, Bolmsjö E, Montelius L, et al. Process development and characterization of antisticking layers on nickel-based stamps designed for nanoimprint lithography. J Vac Sci Technol B 2004;22:3283–7.
[49] Fuchs A, Vratzov B, Wahlbrink T, Georgiev Y, Kurz H. Interferometric in situ alignment for UV-based nanoimprint. J Vac Sci Technol B 2004;22:3242–5.
[50] Sotomayor Torres CM. Alternative lithography. New York: Kluwer; 2003.
[51] Schift H, Bellini S, Gobrecht J, Reuther F, Kubenz M, Mikkelsen MB, et al. Fast heating and cooling in nanoimprint using a spring-loaded adapter in a preheated press. Microelectron Eng 2007;84:932–6.
[52] Guo LJ. Nanoimprint lithography: methods and material requirements. Adv Mater 2007;19:495–513.
[53] Bogdanski N, Wissen M, Mollenbeck S, Scheer HC. Thermal imprint with negligibly low residual layer. J Vac Sci Technol B 2006;24:2998–3001.

[54] Bogdanski N, Wissen M, Ziegler A, Scheer HC. Temperature-reduced nanoimprint lithography for thin and uniform residual layers. Microelectron Eng 2005;78–9:598.
[55] Studer V, Pepin A, Chen Y. Nanoembossing of thermoplastic polymers for microfluidic applications. Appl Phys Lett 2002;80:3614–6.
[56] Chou SY, Krauss PR, Zhang W, Guo LJ, Zhuang L. Sub-10 nm imprint lithography and applications. J Vac Sci Technol B 1997;15:2897–904.
[57] Ansari K, van Kan JA, Bettiol AA, Watt F. Fabrication of high aspect ratio 100 nm metallic stamps for nanoimprint lithography using proton beam writing. Appl Phys Lett 2004;85:476–8.
[58] Hoff JD, Cheng LJ, Meyhofer E, Guo LJ, Hunt AJ. Nanoscale protein patterning by imprint lithography. Nano Lett 2004;4:853–7.
[59] Li HW, Huck WTS. Ordered block-copolymer assembly using nanoimprint lithography. Nano Lett 2004;4:1633–6.
[60] Behl M, Seekamp J, Zankovych S, Sotomayor Torres CM, Zentel R, Ahopelto J. Towards plastic electronics: patterning semi-conducting polymers by nanoimprint lithography. Adv Mater 2002;14:588–91.
[61] Li MT, Wang JA, Zhuang L, Chou SY. Fabrication of circular optical structures with a 20 nm minimum feature size using nanoimprint lithography. Appl Phys Lett 2000;76:673–5.
[62] Zhang W, Chou SY. Fabrication of 60-nm transistors on 4-in. wafer using nanoimprint at all lithography levels. Appl Phys Lett 2003;83:1632–4.
[63] Schift H. Nanoimprint lithography: an old story in modern times? A review. J Vac Sci Technol B 2008;26:458–80.
[64] Schulz H, Scheer HC, Hoffmann T, Sotomayor Torres CM, Pfeiffer K, Bleidiessel G, et al. New polymer materials for nanoimprinting. J Vac Sci Technol B 2000;18:1861–5.
[65] Pfeiffer K, Fink M, Bleidiessel G, Gruetzner G, Schulz H, Scheer HC, et al. Novel linear and crosslinking polymers for nanoimprinting with high etch resistance. Microelectron Eng 2000;53:411–4.
[66] Guo LJ. Recent progress in nanoimprint technology and its applications. J Phys D: Appl Phys 2004;37:R123–41.
[67] Choi P, Fu PF, Guo LJ. Siloxane copolymers for nanoimprint lithography. Adv Funct Mater 2007;17:65–70.
[68] Korczagin I, Lammertink RGH, Hempenius MA, Golze S, Vancso GJ. Surface nano- and microstructuring with organometallic polymers. Adv Polym Sci 2006;200:91–117.
[69] Acikgoz C, Hempenius MA, Vancso GJ, Huskens J. Direct surface structuring of organometallic resists using nanoimprint lithography. Nanotechnology 2009;20:135304.
[70] Manners I. Synthetic metal-containing polymers. New York: Ed. Wiley; 2004.
[71] Kulbaba K, Manners I. Polyferrocenylsilanes: metal-containing polymers for materials science, self-assembly and nanostructure applications. Macromol Rapid Commun 2001;22:711–24.
[72] Khang DY, Yoon H, Lee HH. Room-temperature imprint lithography. Adv Mater 2001;13:749–52.
[73] Matsui S, Igaku Y, Ishigaki H, Fujita J, Ishida M, Ochiai Y, et al. Room temperature replication in spin on glass by nanoimprint technology. J Vac Sci Technol B 2001;19:2801–5.
[74] Matsui S, Igaku Y, Ishigaki H, Fujita J, Ishida M, Ochiai Y, et al. Room-temperature nanoimprint and nanotransfer printing using hydrogen silsequioxane. J Vac Sci Technol B 2003;21:688–92.
[75] Bao LR, Cheng X, Huang XD, Guo LJ, Pang SW, Yee AF. Nanoimprinting over topography and multilayer three-dimensional printing. J Vac Sci Technol B 2002;20:2881–6.
[76] Kehagias N, Reboud V, Chansin G, Zelsmann M, Jeppesen C, Schuster C, et al. Reverse-contact UV nanoimprint lithography for multilayered structure fabrication. Nanotechnology 2007;18:175303.
[77] Pfeiffer K, Reuther F, Fink M, Gruetzner G, Carlberg P, Maximov I, et al. A comparison of thermally and photochemically cross-linked polymers for nanoimprinting. Microelectron Eng 2003;67–8:266–73.
[78] Scheer HC, Schulz H. A contribution to the flow behaviour of thin polymer films during hot embossing lithography. Microelectron Eng 2001;56:311–32.
[79] Tormen M, Romanato F, Altissimo M, Businaro L, Candeloro P, Di Fabrizio EM. Three-dimensional micro- and nanostructuring by combination of nanoimprint and x-ray lithography. J Vac Sci Technol B 2004;22:766–70.
[80] Bender M, Otto M, Hadam B, Vratzov B, Spangenberg B, Kurz H. Fabrication of Nanostructures using a UV-based imprint technique. Microelectron Eng 2000;53:233–6.
[81] Dauksher WJ, Nordquist KJ, Mancini DP, Resnick DJ, Baker JH, Hooper AE, et al. Characterization of and imprint results using indium tin oxide-based step and flash imprint lithography templates. J Vac Sci Technol B 2002;20:2857–61.
[82] Bailey TC, Resnick DJ, Mancini D, Nordquist KJ, Dauksher WJ, Ainley E, et al. Template fabrication schemes for step and flash imprint lithography. Microelectron Eng 2002;61–2:461–7.
[83] Mancini DP, Gehoski KA, Ainley E, Nordquist KJ, Resnick DJ, Bailey TC, et al. Hydrogen silsesquioxane for direct electron-beam patterning of step and flash imprint lithography templates. J Vac Sci Technol B 2002;20:2896–901.
[84] Kim EK, Stacey NA, Smith BJ, Dickey MD, Johnson SC, Trinque BC, et al. Vinyl ethers in ultraviolet curable formulations for step and flash imprint lithography. J Vac Sci Technol B 2004;22:131–5.
[85] Chan-Park MB, Lam YC, Laulia P, Joshi SC. Simulation and investigation of factors affecting high aspect ratio UV embossing. Langmuir 2005;21:2000–7.
[86] Chan-Park MB, Yan YH, Neo WK, Zhou WX, Zhang J, Yue CY. Fabrication of high aspect ratio poly(ethylene glycol)-containing microstructures by UV embossing. Langmuir 2003;19:4371–80.
[87] Jung GY, Ganapathiappan S, Ohlberg DAA, Olynick DL, Chen Y, Tong WM, et al. Fabrication of a 34 x 34 crossbar structure at 50 nm half-pitch by UV-based nanoimprint lithography. Nano Lett 2004;4:1225–9.
[88] Bailey TC, Johnson SC, Sreenivasan SV, Ekerdt JG, Willson CG, Resnick DJ. Step and flash imprint lithography: an efficient nanoscale printing technology. J Photopolym Sci Technol 2002;15:481–6.
[89] Stewart MD, Johnson SC, Sreenivasan SV, Resnick DJ, Willson CG. Nanofabrication with step and flash imprint lithography. J Microlith Microfab Microsys 2005;4:011002.
[90] Resnick DJ, Mancini D, Dauksher WJ, Nordquist K, Bailey TC, Johnson S, et al. Improved step and flash imprint lithography templates for nanofabrication. Microelectron Eng 2003;69:412–9.
[91] Resnick DJ, Sreenivasan SV, Willson CG. Step & flash imprint lithography. Mater Today 2005;8:34–42.
[92] Kettle J, Hoyle RT, Dimov S, Perks RM. Fabrication of complex 3D structures using Step and Flash Imprint Lithography (S-FIL). Microelectron Eng 2008;85:853–5.
[93] Reddy S, Bonnecaze RT. Simulation of fluid flow in the step and flash imprint lithography process. Microelectron Eng 2005;82:60–70.
[94] Scheer HC, Schulz H, Hoffmann T, Sotomayor Torres CM. Problems of the nanoimprinting technique for nanometer scale pattern definition. J Vac Sci Technol B 1998;16:3917–21.
[95] Acikgoz C, Vratzov B, Hempenius MA, Vancso GJ, Huskens J. Nanoscale patterning by UV nanoimprint lithography using an organometallic resist. ACS Appl Mater Inter 2009;1:2645–50.
[96] Lee JN, Park C, Whitesides GM. Solvent compatibility of poly(dimethylsiloxane)-based microfluidic devices. Anal Chem 2003;75:6544–54.
[97] Delamarche E, Schmid H, Michel B, Biebuyck H. Stability of molded polydimethylsiloxane microstructures. Adv Mater 1997;9:741–6.
[98] Bietsch A, Michel B. Conformal contact and pattern stability of stamps used for soft lithography. J. Appl. Phys. 2000;88:4310–8.
[99] Hui CY, Jagota A, Lin YY, Kramer EJ. Constraints on microcontact printing imposed by stamp deformation. Langmuir 2002;18:1394–407.
[100] Kumar A, Whitesides GM. Features of gold having micrometer to centimeter dimensions can be formed through a combination of stamping with an elastomeric stamp and an alkanethiol ink followed by chemical etching. Appl Phys Lett 1993;63:2002–4.
[101] Trimbach D, Feldman K, Spencer ND, Broer DJ, Bastiaansen CWM. Block copolymer thermoplastic elastomers for microcontact printing. Langmuir 2003;19:10957–61.
[102] Csucs G, Künzler T, Feldman K, Robin F, Spencer ND. Microcontact printing of macromolecules with submicrometer resolution by means of polyolefin stamps. Langmuir 2003;19:6104–9.
[103] Williams SS, Retterer S, Lopez R, Ruiz R, Samulski ET, DeSimone JM. High-resolution PFPE-based molding techniques for nanofabrication of high-pattern density, sub-20 nm features: a fundamental materials approach. Nano Lett 2010;10:1421–8.
[104] Rolland JP, Van Dam RM, Schorzman DA, Quake SR, DeSimone JM. Solvent-resistant photocurable "liquid teflon" for microfluidic device fabrication. J Am Chem Soc 2004;126:2322–3.
[105] Xia YN, Zhao XM, Whitesides GM. Pattern transfer: self-assembled monolayers as ultrathin resists. Microelectron Eng 1996;32:255–68.
[106] Xia Y, Kim E, Whitesides GM. Microcontact printing of alkanethiols on silver and its application in microfabrication. J. Electrochem. Soc. 1996;143:1070–9.

[107] Kumar A, Biebuyck HA, Whitesides GM. Patterning self-assembled monolayers: applications in materials science. Langmuir 1994;10:1498–511.
[108] Xia YN, Zhao XM, Kim E, Whitesides GM. A selective etching solution for use with patterned self-assembled monolayers of alkanethiolates on gold. Chem Mater 1995;7:2332–7.
[109] Jeon NL, Clem PG, Payne DA, Nuzzo RG. A monolayer-based lift-off process for patterning chemical vapor deposition copper thin films. Langmuir 1996;12:5350–5.
[110] Jeon NL, Finnie K, Branshaw K, Nuzzo RG. Structure and stability of patterned self-assembled films of octadecyltrichlorosilane formed by contact printing. Langmuir 1997;13:3382–91.
[111] Jeon NL, Choi IS, Whitesides GM, Kim NY, Laibinis PE, Harada Y, et al. Patterned polymer growth on silicon surfaces using microcontact printing and surface-initiated polymerization. Appl Phys Lett 1999;75:4201–3.
[112] Schmitz GJ, Brucker C, Jacobs P. Manufacture of high-aspect-ratio micro-hair sensor arrays. J Micromech Microeng 2005;15:1904–10.
[113] Kim K, Park S, Lee JB, Manohara H, Desta Y, Murphy M, et al. Rapid replication of polymeric and metallic high aspect ratio microstructures using PDMS and LIGA technology. Microsyst Technol 2002;9:5–10.
[114] Odom TW, Love JC, Wolfe DB, Paul KE, Whitesides GM. Improved pattern transfer in soft lithography using composite stamps. Langmuir 2002;18:5314–20.
[115] Choi KM, Rogers JA. A photocurable poly(dimethylsiloxane) chemistry designed for soft lithographic molding and printing in the nanometer regime. J Am Chem Soc 2003;125:4060–1.
[116] Choi DG, Jeong JH, Sim YS, Lee ES, Kim WS, Bae BS. Fluorinated organic-inorganic hybrid mold as a new stamp for nanoimprint and soft lithography. Langmuir 2005;21:9390–2.
[117] Gates BD, Xu QB, Love JC, Wolfe DB, Whitesides GM. Unconventional nanofabrication. Annu Rev Mater Res 2004;34:339–72.
[118] LaFratta CN, Baldacchini T, Farrer RA, Fourkas JT, Teich MC, Saleh BEA, et al. Replication of two-photon-polymerized structures with extremely high aspect ratios and large overhangs. J Phys Chem B 2004;108:11256–8.
[119] Yang SM, Jang SG, Choi DG, Kim S, Yu HK. Nanomachining by colloidal lithography. Small 2006;2:458–75.
[120] Arshady R. Suspension, emulsion, and dispersion polymerization: a methodological survey. Colloid Polym Sci 1992;270:717–32.
[121] Ottewill RH, Shaw JN. Studies on preparation and characterisation of monodisperse polystyrene latices. Part 2: electrophoretic characterisation of surface groupings. Kolloid-Zeitschrift and Zeitschrift Fur Polymere 1967;218:34–40.
[122] Zou DZ, Sun LQ, Aklonis JJ, Salovey R. Model filled polymers. VIII. Synthesis of cross-linked polymeric beads by seed polymerization. J Polym Sci Part A: Polym Chem 1992;30:1463–75.
[123] Stöber W, Fink A, Bohn E. Controlled growth of monodisperse silica spheres in micron size range. J Colloid Interface Sci 1968;26:62–9.
[124] Van Helden AK, Jansen JW, Vrij A. Preparation and characterization of spherical monodisperse silica dispersions in nonaqueous solvents. J Colloid Interface Sci 1981;81:354–68.
[125] Xia YN, Gates B, Yin YD, Lu Y. Monodispersed colloidal spheres: old materials with new applications. Adv Mater 2000;12:693–713.
[126] Dziomkina NV, Vancso GJ. Colloidal crystal assembly on topologically patterned templates. Soft Matter 2005;1:265–79.
[127] Denkov ND, Velev OD, Kralchevsky PA, Ivanov IB, Yoshimura H, Nagayama K. Mechanism of formation of 2-dimensional crystals from latex-particles on substrates. Langmuir 1992;8:3183–90.
[128] Trau M, Sankaran S, Saville DA, Aksay IA. Electric-field-induced pattern-formation in colloidal dispersions. Nature 1995;374:437–9.
[129] Dziomkina NV, Hempenius MA, Vancso GJ. Symmetry control of polymer colloidal monolayers and crystals by electrophoretic deposition onto patterned surfaces. Adv Mater 2005;17:237–40.
[130] Besra L, Liu M. A review on fundamentals and applications of electrophoretic deposition (EPD). Prog Mater Sci 2007;52:1–61.
[131] Gates B, Qin D, Xia YN. Assembly of nanoparticles into opaline structures over large areas. Adv Mater 1999;11:466–9.
[132] Aizenberg J, Braun PV, Wiltzius P. Patterned colloidal deposition controlled by electrostatic and capillary forces. Phys Rev Lett 2000;84:2997–3000.
[133] Zheng HP, Lee I, Rubner MF, Hammond PT. Two component particle arrays on patterned polyelectrolyte multilayer templates. Adv Mater 2002;14:569–72.
[134] Xia YN, Yin YD, Lu Y, McLellan J. Template-assisted self-assembly of spherical colloids into complex and controllable structures. Adv Funct Mater 2003;13:907–18.
[135] Kondo M, Shinozaki K, Bergstrom L, Mizutani N. Preparation of colloidal monolayers of alkoxylated silica particles at the air-liquid interface. Langmuir 1995;11:394–7.
[136] Wickman HH, Korley JN. Colloid crystal self-organization and dynamics at the air/water interface. Nature 1998;393:445–7.
[137] Aveyard R, Clint JH, Nees D, Paunov VN. Compression and structure of monolayers of charged latex particles at air/water and octane/water interfaces. Langmuir 2000;16:1969–79.
[138] Fulda KU, Tieke B. Langmuir films of monodisperse 0.5 μm spherical polymer particles with a hydrophobic core and a hydrophilic shell. Adv Mater 1994;6:288–90.
[139] Wang DY, Möhwald H. Rapid fabrication of binary colloidal crystals by stepwise spin-coating. Adv Mater 2004;16:244–7.
[140] Deckman HW, Dunsmuir JH. Natural lithography. Appl Phys Lett 1982;41:377–9.
[141] Fischer UC, Zingsheim HP. Sub-microscopic pattern replication with visible-light. J Vac Sci Technol B 1981;19:881–5.
[142] Hulteen JC, Van Duyne RP. Nanosphere lithography: a materials general fabrication process for periodic particle array surfaces. J Vac Sci Technol A 1995;13:1553–8.
[143] Kempa K, Kimball B, Rybczynski J, Huang ZP, Wu PF, Steeves D, et al. Photonic crystals based on periodic arrays of aligned carbon nanotubes. Nano Lett 2003;3:13–8.
[144] Wang XD, Summers CJ, Wang ZL. Large-scale hexagonal-patterned growth of aligned ZnO nanorods for nano-optoelectronics and nanosensor arrays. Nano Lett 2004;4:423–6.
[145] Veinot JGC, Yan H, Smith SM, Cui J, Huang QL, Marks TJ. Fabrication and properties of organic light-emitting "nanodiode" arrays. Nano Lett 2002;2:333–5.
[146] Kuo CW, Shiu JY, Chen PL. Size- and shape-controlled fabrication of large-area periodic nanopillar arrays. Chem Mater 2003;15:2917–20.
[147] Michel R, Reviakine I, Sutherland D, Fokas C, Csucs G, Danuser G, et al. A novel approach to produce biologically relevant chemical patterns at the nanometer scale: selective molecular assembly patterning combined with colloidal lithography. Langmuir 2002;18:8580–6.
[148] Tan BJY, Sow CH, Lim KY, Cheong FC, Chong GL, Wee ATS, et al. Fabrication of a two-dimensional periodic non-close-packed array of polystyrene particles. J Phys Chem B 2004;108:18575–9.
[149] Johnson SA, Ollivier PJ, Mallouk TE. Ordered mesoporous polymers of tunable pore size from colloidal silica templates. Science 1999;283:963–5.
[150] Trujillo NJ, Baxamusa SH, Gleason KK. Grafted functional polymer nanostructures patterned bottom-up by colloidal lithography and initiated chemical vapor deposition (iCVD). Chem Mater 2009;21:742–50.
[151] Acikgoz C, Ling XY, Phang IY, Hempenius MA, Reinhoudt DN, Huskens J, et al. Fabrication of freestanding nanoporous polyethersulfone membranes using organometallic polymer resists patterned by nanosphere lithography. Adv Mater 2009;21:2064–7.
[152] Kosiorek A, Kandulski W, Glaczynska H, Giersig M. Fabrication of nanoscale rings, dots, and rods by combining shadow nanosphere lithography and annealed polystyrene nanosphere masks. Small 2005;1:439–44.
[153] Haginoya C, Ishibashi M, Koike K. Nanostructure array fabrication with a size-controllable natural lithography. Appl Phys Lett 1997;71:2934–6.
[154] Choi DG, Yu HK, Jang SG, Yang SM. Colloidal lithographic nanopatterning via reactive ion etching. J Am Chem Soc 2004;126:7019–25.
[155] Itani T, Wakamiya W, Cashmore J, Gower M. 157-nm Lithography with high numerical aperture lens for sub-70 nm node. Microelectron Eng 2003;67–8:39–46.
[156] Wu B, Kumar A. Extreme ultraviolet lithography: towards the next generation of integrated circuits. Opt Photon Focus 2009;7:4.
[157] Yu A, Liu H, Blinco JP, Jack KS, Leeson M, Younkin TR, et al. Patterning of tailored polycarbonate based non-chemically amplified resists using extreme ultraviolet lithography. Macromol Rapid Commun 2010;31:1449–55.
[158] Morecroft D, Yang JKW, Schuster S, Berggren KK, Xia Q, Wu W, et al. Sub-15 nm nanoimprint molds and pattern transfer. J Vac Sci Technol B 2009;27:2837–40.

[159] Wu W, Tong WM, Bartman J, Chen Y, Walmsley R, Yu Z, et al. Sub-10 nm nanoimprint lithography by wafer bowing. Nano Lett 2008;8:3865–9.
[160] Glinsner T, Kreindl G, Kast M. Nanoimprint lithography. The technology makes its mark on CMOS image sensors and in the nano-world. Optik Photonik 2010;2:42–5.
[161] Peroz C, Dhuey S, Volger M, Wu Y, Olynick D, Cabrini S. Step and repeat UV nanoimprint lithography on pre-spin coated resist film: a promising route for fabricating nanodevices. Nanotechnology 2010;21:1–5.
[162] Perl A, Reinhoudt DN, Huskens J. Microcontact printing: limitations and achievements. Adv Mater 2009;21:2257–68.
[163] Shestopalov AA, Clark RL, Toone EJ. Inkless microcontact printing on SAMs of Boc- and TBS-protected thiols. Nano Lett 2010;10:43–6.
[164] Xia Y, Qin D, Whitesides GM. Microcontact printing with a cylindrical rolling stamp: a practical step toward automatic manufacturing of patterns with submicrometer-sized features. Adv Mater 1996;8:1015–7.
[165] Stagnaro, A. Development of a roll-to-roll machine for continuous high-speed microcontact printing. PhD thesis. Massachusetts Institute of Technology; 2008.
[166] Jiang P, Bertone JF, Colvin VL. A lost-wax approach to monodisperse colloids and their crystals. Science 2001;291:453–7.
[167] Chen X, Chen ZM, Fu N, Lu G, Yang B. Versatile nanopatterned surfaces generated via three-dimensional colloidal crystals. Adv Mater 2003;15:1413–7.
[168] Fischer UC, Zingsheim HP. Sub-microscopic pattern replication with visible-light. J Vac Sci Technol 1981;19:881–5.
[169] Knoll AW, Pires D, Coulembier O, Dubois P, Hedrick JL, Frommer J, et al. Probe-based 3-D nanolithography using self-amplified depolymerization polymers. Adv Mater 2010;22:3361–5.
[170] Pires D, Hedrick JL, De Silva A, Frommer J, Gotsmann B, Wolf H, et al. Nanoscale three-dimensional patterning of molecular resists by scanning probes. Science 2010;328:732–5.

Canet Acikgoz obtained her MSc from Middle East Technical University (Turkey) after working on the use of Fischer carbenes in the synthesis of cycloheptadienones incorporating ferrocenyl moiety in the group of Prof. Metin Zora. Subsequently she moved to Twente University (The Netherlends) to obtain her PhD under the supervision of Profs. Dr. Jurriaan Huskens and Dr. Julius Vancso for the thesis titled: Controlled polymer nanostructures by alternative lithography. Since April 2010 she has been working as a postdoctoral fellow at ETH Zurich with Prof. Marcus Textor on the development of nonfouling and antimicrobial surface platforms.

Mark Hempenius studied chemistry at the University of Leiden, The Netherlands and obtained a PhD in chemistry at the same university. At present he is Assistant Professor at the Department of Polymer Materials Science and Technology at the University of Twente, The Netherlands. Research interests include controlled polymerizations and organometallic polymer chemistry.

Jurriaan Huskens studied chemical engineering at the Eindhoven University of Technology, The Netherlands. He obtained his PhD with Prof. Herman van Bekkum and Dr. Joop A. Peters from the Delft University of Technology, The Netherlands, in 1994, on a thesis on the coordination and homogeneous catalysis of lanthanides. After postdoctoral stays with Prof. A. Dean Sherry (University of Texas at Dallas) and Prof. Manfred T. Reetz (Max-Planck-Institut für Kohlenforschung, Mülheim an der Ruhr, Germany), he became Assistant Professor in the group of Prof. David N. Reinhoudt at the University of Twente, The Netherlands, in 1998 and Associate Professor in March 2003. He has been appointed Full Professor "Molecular Nanofabrication" at the University of Twente, The Netherlands, in September 2005. Present research interests encompass: supramolecular chemistry at interfaces, multivalency, bottom-up nanofabrication, nanolithography, and the integration of top-down and bottom-up nanofabrication techniques. He is a recipient of the Unilever Research Award 1990, of a Marie Curie fellowship (1997), of the Gold Medal 2007 of the Royal Netherlands Chemical Society, and of a "Vernieuwingsimpuls Vici" grant (2008).

G. Julius Vancso studied physics and materials science at the University of Budapest, Hungary, and at the Swiss Federal Institute of Technology (ETH-Zürich) and holds a PhD in solid state physics. He is at present Professor and Chairholder in Polymer Materials Science and Technology at the University of Twente in the Netherlands, and carries out his research in the MESA^{+} Institute for Nanotechnology of the same university. His current interests involve nanofabrication with stimulus responsive macromolecules, single molecule studies (AFM, photonics), integration of polymer-semiconductor-metal nanostructures for function, surface engineering, and materials chemistry of organometallic polymers. Julius Vancso holds an adjunct professorship at Nanyang Technological University in Singapore, is external member of the Hungarian Academy of Sciences, and is Fellow of the Royal Society of Chemistry of the UK.